Tissue engineered scaffolds for corneal endothelial regeneration : a material's perspective

Tissue engineered scaffolds for corneal endothelial regeneration: A material's perspective

Jasper Delaey[1]*, Lobke De Vos[1]*, Carina Koppen[2,3], Peter Dubruel[1], Sandra Van Vlierberghe[1], Bert Van den Bogerd[2**]

*These authors contributed equally to this manuscript

[1] Polymer Chemistry & Biomaterials Group, Centre of Macromolecular Chemistry (CMaC), Department of Organic and Macromolecular Chemistry, Ghent University, Ghent (Belgium)
[2] Antwerp Research Group for Ocular Science (ARGOS), Translational Neurosciences, Faculty of Medicine, University of Antwerp, Wilrijk, Belgium
[3] Department of Ophthalmology, Antwerp University Hospital, Edegem, Belgium

**bert.vandenbogerd@uantwerpen.be

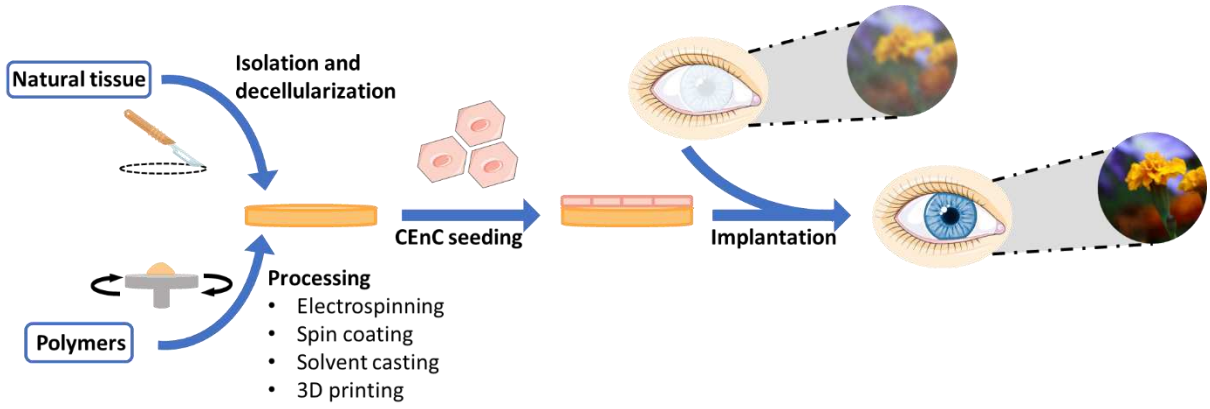

Abstract

Currently, the treatment of corneal diseases caused by damage to the corneal endothelium requires a donor cornea. Because of their limited availability (1 donor cornea for 70 patients in need), researchers are investigating alternative approaches that are independent of donor tissue. One of them includes the development of a tissue engineered scaffold onto which corneal endothelial cells are seeded. In order to function as a suitable substrate, some of its essential properties including thickness, permeability, transparency and mechanical strength should meet certain demands. Additionally, the membrane should be biocompatible and allow the formation of a functional endothelium on the surface. Many materials have already been investigated in this regard including natural, semi-synthetic and synthetic polymers. In the current review, we present an overview of their characteristics and provide a critical view on the methods exploited for material characterization. Next, also the suitability of scaffolds to serve their purpose is discussed along with an overview of natural tissues (e.g. amniotic membrane and lens capsule) previously investigated for this application. Eventually, we

propose a consistent approach to be exploited ideally for membrane characterization in future research. This will allow a scientifically sound comparison of materials and membranes investigated by different research groups, hence benefitting research towards the creation of a suitable/optimal tissue engineered endothelial graft.

Table of content

1. Introduction

The cornea is the transparent window of the eye lying in front of the iris and pupil and is the major refractive element of the eye. Trauma or disease can lead to an opaque cornea and concomitantly, visual impairment and even blindness. Corneal blindness, a collective term grouping all conditions that result in a dysfunctional cornea, is the 4th leading cause of global blindness, affecting around 23 million people.[1,2]

Histologically, it is a 500 µm thin tissue that harbours three corneal cell layers separated by two acellular membranes (Figure 1). Between the cornea and the iris, there is a fluid filled cavity known as the anterior chamber.[3] The most superficial layer of the cornea is the stratified squamous corneal epithelium that acts as a barrier to intruders such as microorganisms or dust particles. The epithelium lies on top of Bowman's layer, which separates it from the corneal stroma. The stroma is the thickest corneal layer, forming up to 90% of corneal thickness, and is composed of very strictly organised collagen lamellae containing dispersed quiescent keratocytes. Underneath lies the corneal endothelium and its basement membrane, being the Descemet's membrane (DM). The corneal endothelial cells (CEnCs) form a single layer of hexagonally shaped cells that have the primary function to regulate the corneal hydration rate, which is directly correlated with corneal transparency. By means of an osmotic pressure from the stroma to the anterior chamber, the endothelial cells counteract the passive diffusion of water and nutrients from the anterior chamber towards the corneal stroma. To maintain this osmotic gradient, the endothelial cells contain Na^+/K^+-ATPase pumps that pump Na^+ and K^+ ions from stroma towards the anterior chamber. The resulting concentration difference in ions creates an osmotic gradient which in turn will cause a flow of fluid from the stroma towards the anterior chamber. This mechanism maintains the relative deturgescence of the stroma which is important for its transparency.[4]

Corneal endothelial cells cannot regenerate, which is why the total cell density only declines throughout life, even in healthy individuals, although without affecting their sight. However, when the cell density is situated below an approximate threshold of 500 cells/mm^2, either due to corneal disease or trauma, the cells cannot oppose the passive water influx into the cornea which leads to corneal oedema and subsequent scattering of the incoming light. Macroscopically, the cornea of such patients looks opaque which results in visual impairment. Corneal endothelial dysfunction is the most prevalent indication for corneal transplantation, representing 40% of all keratoplasties.

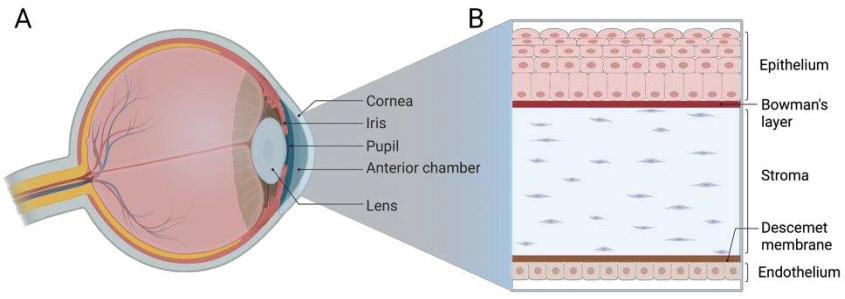

Figure 1: (A) a cross-section of an eye with (B) an enlargement of the cornea, indicating the 5 different layers.

The only option for these patients is a corneal endothelial transplantation during which the diseased corneal endothelium is replaced by an endothelial layer derived from a cadaveric donor cornea. Currently, two prominent techniques are used, namely Descemet's membrane endothelial keratoplasty (DMEK) and Descemet stripping automated endothelial keratoplasty (DSAEK). In the former, the Descemet's membrane and the endothelial layer are transplanted, while the latter also contains part of the stroma. While clinical results are very satisfying, a global donor shortage limits treatment for every patient. Even in countries with a well-established cornea bank system, the demand is chronically higher than the supply.[5] For tissue donation, the majority of donors is excluded because they suffer from systemic or infectious diseases that may be transmitted to the patient.[6] That is why researchers are looking for alternative treatments, such as stimulating the *in vivo* regeneration (possibly by additional pharmacological stimulation)[3], alternative tissue preparation[7], endothelial cell injection[8] or by tissue engineering an endothelial graft[9–12]. Both cell-based approaches (i.e. the cell injection and tissue engineered endothelium) are based on the rationale to grow corneal endothelial cells from one donor in high numbers ex vivo to treat multiple patients with only one donor cornea, thereby shortening the current waiting lists. The use of allogeneic cells is attainable since currently corneal transplantation is also performed with allogeneic tissue without any tissue matching.[13] In fact, the cornea can be considered as an immune-privileged site, also known as anterior chamber associated immune deviation, where antigen-specific systemic tolerance is established upon foreign antigen (e.g. cells, tissue, biomaterials, etc.) introduction in the anterior chamber.[14]

The cell-injection method to recreate the corneal endothelium comprises the injection of CEnCs in suspension in the anterior chamber of the cornea after which they should attach to the stroma when placing the patient face down.[12] During the first-in-human clinical study performed by Kinoshita *et al.*, 11 patients were injected with $1x10^6$ cells and after 24 weeks, endothelial cell density of the patients ranged from 947 to 2,833 cells/mm^2.[8] Although the authors did not observe any undesired side effects such as elevated intraocular pressure, it is questioned what happens exactly with the majority of the cells that do not attach. On the other hand, when cells are cultured on a scaffold, they are grafted directly onto their final destination, similar to a corneal endothelial transplantation. Moreover, a tissue engineered endothelium allows for direct control over the final cell density that is transplanted. For instance, hypercellularized grafts can be fabricated with high endothelial cell densities which can result in long-term success of the graft. Furthermore, a tissue engineered endothelium is similar to current endothelial grafts for transplantation and as such, the surgical procedure to implant the scaffolds would be similar to the currently applied methods. This can facilitate the implementation of the cell therapy as soon as a suitable scaffold is developed. A scaffold is considered a structural support for cell attachment and tissue development (if necessary) that mimics the function of the native extracellular matrix (ECM).[15] There exist several types of scaffolds but this review mainly focusses on the design of a scaffold to facilitate endothelial cell transplantation.

Already in 1978, the hypothesis of a tissue engineered graft was coined, but no effective scaffold has reached the clinic yet.[15] Throughout the years, the reports on corneal endothelial scaffolds range from fully biological scaffolds, to semi-synthetic and synthetic materials. The underlying reason for the cumbersome clinical translation is twofold: primary corneal endothelial cells are difficult to grow and the perfect scaffold, or cell carrier, for these cells is still lacking.[16,17] Even though the corneal endothelium is a 2D tissue that is quite simple in its build-up, a proper scaffold for corneal endothelial tissue engineering must display intricate properties with regard to both cell compatibility and subsequent surgical transplantation in

patients. Recently, Jameson et al. have summarized recent developments regarding cell-based research on endothelial scaffolds through *in vitro* and *in vivo* models.[18]
Although biological membranes have shown promising results, the use of (semi-)synthetic building blocks to create tissue scaffolds is interesting since this offers complete control over the manufacturing process while the different properties (Young's modulus, thickness, permeability, transparency, topography, biodegradability) can be tuned. Therefore, it is interesting to scrutinize the published reports on (semi-)synthetic scaffolds and compare them to the natural corneal endothelial cell scaffold, namely the Descemet's membrane. While other literature reviews in this field focus on a qualitative description of the material classes and their interaction with endothelial cells, we bring quantitative material characteristics of corneal endothelial scaffolds to attention from a material scientist's point of view. In this review, we elaborate on the essential properties of a corneal endothelial cell scaffold for transplantation purposes, namely permeability, porosity, thickness, mechanical strength and transparency.

2. Properties of the natural Descemet's membrane

The Descemet's membrane is an acellular tissue located at the posterior side of the cornea and secreted by corneal endothelial cells. The major components of the Descemet's membrane include laminin, fibronectin, collagen type IV & VIII, nidogen and perlecan.[19–21] Two distinct layers can be identified in the Descemet's membrane. The first, anterior layer has a banded structure and is fully secreted by the time of birth. The second, posterior layer is deposited by the corneal endothelial cells during life and has a homogeneous, non-banded, appearance.[22] A slight difference in composition between these layers has been identified. More specifically, the banded layer is mainly comprised of collagen VIII and proteoglycans while the non-banded layers have a more homogeneously distributed composition as opposed to the banded pattern.[19] A review about the structure of the Descemet's membrane, its function, development and regeneration was recently published by Oliveira *et al*.[19]
The Descemet's membrane acts as the basement membrane for the corneal endothelial cells within the human cornea. Therefore, the properties of this membrane can be regarded as a benchmark for scaffolds which fulfil a similar function after implantation. One can argue that artificial scaffolds that comply with these characteristics will be the most similar to the natural Descemet's membrane and will therefore have the best chance of being successful upon transplantation.

A first important property includes permeability. Since the cornea is not vascularized, nutrients and waste products need to be able to diffuse from the anterior chamber through the Descemet's membrane.[19] Unfortunately, there is only little reported about the permeability of the human Descemet's membrane while for rabbits, there are more data available. The permeability of rabbit endothelium and Descemet's membrane are listed in Table 1. A study performed by Kim *et al.* shows an interesting relationship between the molar mass of a compound and its permeability through the rabbit Descemet's membrane and endothelium.[23] The higher molar masses exhibit exponentially less diffusivity compared to low molar masses. Assuming this trend holds true for human Descemet's membrane indicates that researchers should primarily focus on the diffusion of lower molar mass compounds. Indeed, glucose, a low molecular weight molecule, is considered to be the principal compound for energy delivery

in the cornea.[24] However, one has to be careful when comparing the animal Descemet's membrane with that of humans, since animals are usually significantly younger and the Descemet's membrane's thickness, and thus resistance to diffusion, increases with age.[25] Nonetheless, the permeability of compounds tested both in humans and rabbits appears to be within the same order of magnitude.[26] When considering fluorescein, being a relatively small molecule (0.3 kDa), the permeability through the human cornea is $(3.0\text{-}4.0 \pm 0.5)\times10^{-6}$ cm/s while that for the rabbit is $(5.1\pm0.8)\times10^{-6}$ cm/s.[26,27] Fluorescein is also one of the only components which has been tested in human *in vivo* studies, since this is part of the routine examination at ophthalmology departments.
However, it can be anticipated that it will not be an issue if a synthetic Descemet's membrane would be more permeable than the natural Descemet's membrane, since the cellular endothelial layer with its cortical belt of tight junctions is considered to be the limiting layer for diffusion. This is clear from studies on rabbit Descemet's membrane with and without the corneal endothelium present using mannitol as a model compound with the former having a permeability of $(7.0\pm0.5)\times10^{-6}$ cm/s and the latter being almost two times more permeable (i.e. permeability of $(1.2\pm0.1)\times10^{-5}$ cm/s).[23]
Another property of the Descemet's membrane, which might be related to its permeability, is its porosity. Using scanning electron microscopy (SEM), the human Descemet's membrane was found to have an average pore size of 38 nm.[28] However, since SEM is usually performed under dehydrated conditions, the observed pore size might be over or underestimated due to dehydration of the Descemet's membrane during sample preparation.[29]
The thickness is also one of the important characteristics and is per definition related to the permeability. It is a property that is highly dependent on the age of the person and ranges from 2 µm to 10 µm.[22] Important here is to make the distinction between at birth and is on average 3 µm thick, while the latter is deposited during aging and contributes to an average total thickness of the Descemet's membrane of 10 µm by the end of a person's life. [22]
The thickness of DSAEK and DMEK transplants are also listed in Table 1. Both are currently used to treat a diseased corneal endothelium and are therefore a good reference for synthetic scaffolds. Having implants that are not too thick is important when one wants to limit refractive effects. Moreover, it was shown that corneal higher-order aberrations after keratoplasty were significantly less in patients receiving DMEK surgery compared to patients receiving DSAEK surgery.[30] This result might be due to a difference in graft thickness, asymmetrically cut grafts or decentrally positioned grafts in the case of DSAEK, highlighting the importance of thinner grafts.[30,31] However, one of the few relevant objections to DMEK is that the unpredictable scrolling behaviour of the Descemet's membrane can make the preparation of the graft and its unfolding in the anterior chamber complicated leading to an early loss of transplanted cells. DSAEK in contrast allows for a more standardised surgical course since the supporting stroma provides a thicker graft that is much more easy to handle; this explains a lower incidence of peri-operative complications.[32] Here, synthetic membranes can be improved over the natural transplant, since they can be made in a standardised way and issues such as the scrolling behaviour can be avoided or tuned as desired.

The mechanical properties of the Descemet's membrane can be considered very relevant, both with regard to cellular response, as described in section 3.5 3.5, as well as for surgical handling. The latter being a more qualitative estimation but nonetheless important. It should be noted that the reported values for the mechanical properties of the Descemet's membrane differ significantly depending on the study. Typically reported values for the Young's modulus range from 0.23 kPa to 2.57 MPa.[25,28,33,34] In Table 1 both the Young's modulus and the

stiffness are reported. While they are similar, Young's modulus (E [Pa], equation 1) is expressed as a change in force per area (F/A) divided by the change in strain (i.e. the total elongation over the original length (dL/L_0) while stiffness (k [N/m], equation 2) is a change in force divided by elongation. It should be noted that the varying values are a consequence of the methodology employed when measuring the membranes, since different techniques often result in different values while hydration of the membranes also plays an important role in the final result. Moreover, variations can also result from compositional differences as well as age-dependent differences in thickness.

$$E = \frac{\sigma}{\varepsilon} = \frac{\frac{F}{A}}{\frac{dL}{L_0}} \quad (1)$$

$$k = \frac{F}{dL} \quad (2)$$

Since the transmittance of light through the cornea is essential, the last important characteristic is transparency. The Descemet's membrane is highly transparent (90%) in the visual range.[9] This value is similar to the transparency of the complete cornea in the same region (≥ 90%), while the cornea is almost completely opaque under wavelengths of 300 nm. A comparable measurement for the individual Descemet's membrane could not be found but it is unlikely that this opacity towards UV-light is significantly influenced by the Descemet's membrane, considering the multitude of layers present in the cornea, many of which are significantly thicker than the Descemet's membrane.[35]

While the properties of the healthy Descemet's membrane can act as a positive control, the diseased Descemet's membrane might be employed as negative control, mainly indicating cellular properties that are less desirable. As reference, the Descemet's membrane from patients with Fuchs' endothelial corneal dystrophy (FECD) might be the most relevant since it is responsible for 80% of the required corneal endothelial transplantations and even 40% of all corneal transplantations.[36] It is characterized by the formation of guttae on the Descemet's membrane (i.e. malformations that grow between the endothelial cells) and causes accelerated loss of the corneal endothelial cells. This leads to corneal oedema, which in turn results in corneal opacification and visual impairment.[37,38] Elhalis *et al.* have discussed this disease in an excellent review.[37]

The molecular composition of the diseased Descemet's membrane is largely comparable to the healthy Descemet's membrane. However, when considering the thickness, it has been shown that the former can be up to 37% thicker than its healthy equivalent.[39]. Additionally, it was found that the wide-spaced collagen is softer in diseased Descemet's membrane compared to in healthy Descemet's membrane (Table 1).[40]

Table 1: overview of the properties of the cornea, Descemet's membrane and corneal endothelium.

Notes	Cornea	Notes	Descemet's membrane	Notes	Corneal Endothelium	Notes	References
Permeability	**cm^2/s**		**cm/s**		**cm/s**		
Glucose	1.0×10^{-7}-3.0×10^{-6}	Diffusion coefficient					[24,41,42]
Mannitol			$1.2 \pm 0.1 \times 10^{-5}$*		$7.0 \pm 0.5 \times 10^{-6}$*	Including DM and part of stroma	[23]
Fluorescein					$3.0\text{-}4.0 \times 10^{-6}$	*In vivo*	[26,27]
					$5.1 \pm 0.8\ 10^{-6}$ *	*In vivo*	[26]
Sucrose					$4.5 \pm 0.7 \times 10^{-6}$*		[23]
Dextran A (15-17 kDa)					$5.8 \pm 0.7 \times 10^{-7}$ *		[23]
Dextran B (60-90 kDa)					$8.1 \times 1.4 \times 10^{-8}$*		[23]
Albumin	1.0×10^{-7}						[41,42]
Young's modulus			**MPa**		**MPa**		
			$50 \pm 17.8 \times 10^{-3}$	AFM, hydrated	$4{,}1 \pm 1.7 \times 10^{-3}$*	AFM	[28,34]
			$0.23\text{-}2.6 \times 10^{-3}$	AFM, hydrated			[33]
			$11.7 \pm 7.4 \times 10^{-3}$*	AFM			[34]
			2.57±0.37	Tensile			[25]
Stiffness			**MPa**				

			2.57 ± 0.37	Tensile, hydrated, healthy			[25]
			4.8 ± 1.2 x 10^3	AFM, dehydrated, healthy			[40]
			3.6 ± 0.3 x 10^3	AFM, dehydrated, wide spaced collagen, FECD			[40]
			4.4 ± 0.3 x 10^3	AFM, dehydrated, FECD			[40]
			1.8 ± 0.8	AFM, hydrated, healthy			[40]
			1.0 ± 0.7	AFM, hydrated, wide spaced collagen, FECD			[40]
			2.0 ± 0.7	AFM, hydrated, FECD			[40]
Thickness	**µm**		**µm**				
Total	534		10.2 ± 0.4	Electronic length gauge, hydrated			[25]
Banded layer			2.2-4.5	SEM			[22]
Non-banded layer			2-10	SEM			[22]
DSAEK graft	100-200						[41,42]
DMEK graft	14-20						[43]
Transparency	**%**	**nm**	**%**				
	>90	500-1300	>90	Spectrophotometry (405, 450, 490, 530, 630 nm)			[9]
	80	380					[44]
	>95	600-1000					[44]

Porosity			**nm**				
			38	SEM			[28]

*Values from rabbit

3. Discussion of properties of the tissue engineered scaffolds and its materials

Despite the high success rate of the DMEK and DSAEK surgery, the shortage of the donor corneas remains a hurdle. To tackle this issue, researchers have attempted to find more readily available alternatives for donor corneas. One of the approaches include the development of a tissue engineered scaffold on which *ex vivo* expanded corneal endothelial cells can be seeded to replace the diseased DM and endothelium. As visualised in Figure 2, two approaches can be distinguished, either using membranes or films which are isolated from the ECM of natural sources (e.g. lens capsule, fish scales, amniotic membrane) or making a completely new scaffold constituting polymers. The latter includes natural (e.g. collagen, gelatin, etc.), semi-synthetic (e.g. blend of chitosan with PEG or PCL, etc.) and synthetic (e.g. PCL, PMMA, PDLLA, etc.) polymers. In the following section, the methods and results of tissue engineered scaffolds from polymers as well as some of the natural membranes will be discussed from a material scientist's point of view. The characteristics will be compared to those of the natural DM.

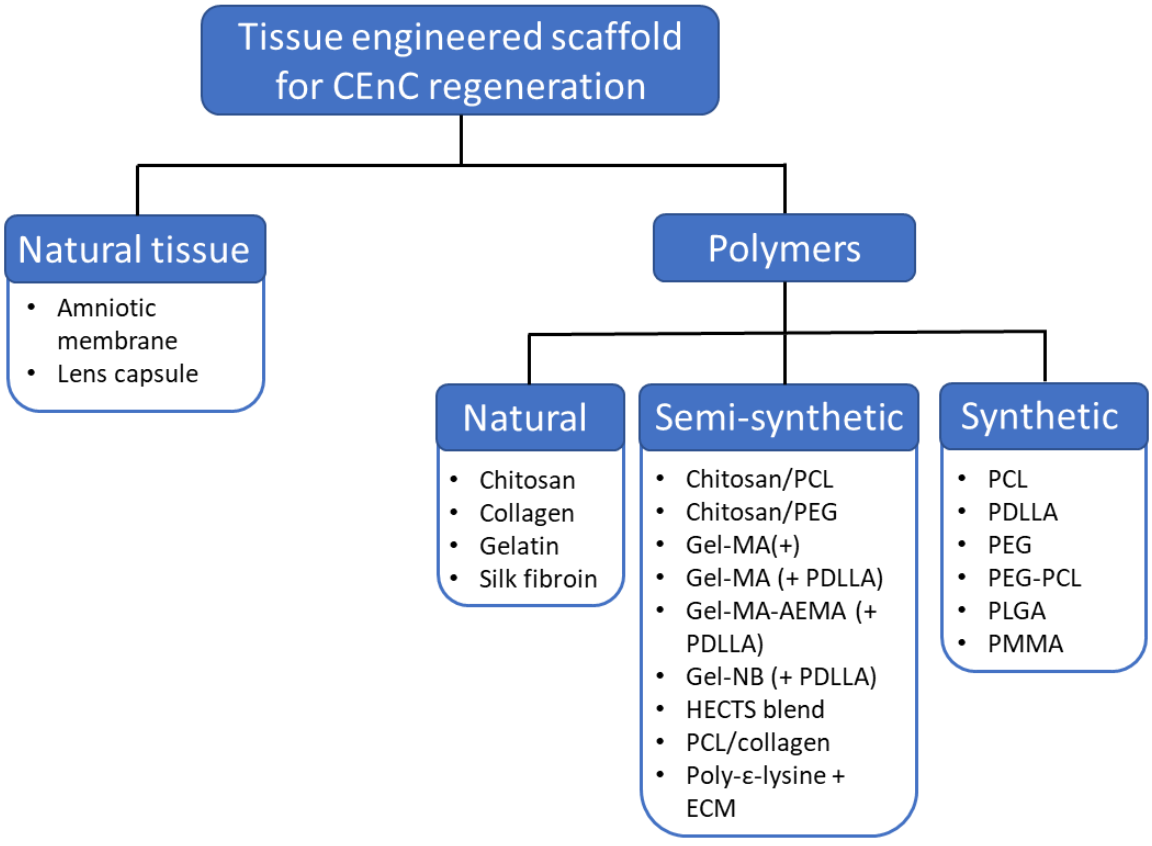

Figure 2. visual overview of the types of materials investigated as scaffold for corneal endothelial regeneration.

Polymers can be divided into three categories based on their origin and composition: natural, semi-synthetic and synthetic. Natural polymers are materials extracted from natural sources such as plants, animals and microorganisms.[45,46] Examples of this type are macromolecules

built up from proteins (e.g. collagen) or polysaccharides (e.g. alginate, starch and chitosan). This class of polymers is appealing for biomedical applications because they are biocompatible, biodegradable and have a low or no cytotoxicity.[47] Additionally, they frequently resemble the ECM, which is often desirable in the biomedical field. However, there are some disadvantages to this material class. Due to natural variability, natural polymers suffer from batch-to-batch differences meaning that polymers derived from the same source can have inconsistent properties.[48] Additionally, nature-derived materials might be immunogenic or transfer pathogens. The production of naturally sourced polymers, while often at low cost, depends on environmental factors which are difficult to control, making this a relatively slow process.[49,50] Also, the thermal and mechanical properties of natural polymers are not suitable to support some biomedical (manufacturing) applications. Collagen type I, which has been screened for corneal tissue engineering, lacks mechanical strength needed for suturing, for example.[51]

In an attempt to circumvent these issues, synthetic polymers have been investigated as alternative to serve biomedical applications.[52] Polymers are considered synthetic when the essential building blocks cannot be extracted from natural sources and should be synthetically created by human intervention. The production of a synthetic polymer is highly reproducible, eliminating the batch-to-batch variations concomitant with natural polymers and providing predictable physical and chemical properties. In most cases, larger quantities can be synthesised compared to natural polymers. Examples include poly(ethylene terephthalate) (PET), poly(ε-caprolactone) (PCL) and poly(methylmethacrylate) (PMMA). The properties of synthetic polymers can be easily tuned to the desired properties.[48] Care must be taken when applying these materials for biomedical applications, as they are not derived from natural sources and thus not necessarily biocompatible, some polymers can trigger an immunogenic response. Although, a wide variety of synthetic polymers have already been successfully applied in the biomedical field, with or without a cell-interactive coating.[53] Additionally, both degradable and non-degradable synthetic polymers exist, which should be taken into account when selecting a polymer for a specific biomedical application. A degradable material is frequently investigated as (part of a) tissue engineered scaffold for corneal endothelial regeneration because the CEnCs produce their own basement membrane which is anticipated to replace the degrading scaffold.

To tune the properties of natural polymers towards certain values, they can be combined or modified with synthetic compounds or polymers. The natural and synthetic components can be mixed to form a blend or chemically linked with each other to create e.g. a copolymer. In this case, we refer to the polymer as semi-synthetic rather than natural. To exemplify, collagen is a natural polymer that can be found in the ECM and which can be extracted from skin, bones, etc. When mixed with the synthetic PCL, a semi-synthetic PCL/collagen blend is formed. Semi-synthetic polymers offer the possibility to customize the properties towards the requirements of a certain application. When a semi-synthetic polymer is combined with a synthetic polymer, it also belongs to the semi-synthetic class.

To obtain a polymer in a useful shape or structure from its solution or melt, multiple polymer processing techniques exist. To produce membranes for ocular applications, the four main techniques that are mentioned in literature are solvent casting, spin coating, electrospinning and 3D bioprinting (Figure 3). In solvent casting, a polymer solution is introduced into a mould exhibiting a certain shape after which the solvent is evaporated to create a polymer

membrane.[42] A similar membrane is produced by means of spin coating, in which the polymer solution is subjected to rapid rotation which allows the solvent to evaporate and the polymer to spread out.[10] Parameters, such as the rotation speed, can be altered to change the thickness of the scaffold. With electrospinning, a scaffold consisting of micro- and nanoscale fibres is formed from a polymeric solution.[54,55] Herein, a syringe pump is loaded with a syringe containing a polymer solution and connected to a needle with a certain diameter. A feed rate is established and by switching on the voltage supply, generally ranging from 5 to 20 kV, an electrical field is established between the needle and the metal collector. This results in an accumulation of charges on the surface of the polymer droplet at the tip of the needle. When the electrical field reaches a certain critical value, the repulsive forces overcome the surface tension and the droplet forms a conically shaped structure known as a Taylor cone. Then, the polymer solution is further stretched into an electrically charged polymer jet which is drawn towards the oppositely charged collector while the solvent evaporates. This results in a sheet of randomly distributed fibres on the collector plate. Electrospinning is a versatile technique in which a lot of parameters, including the feed rate, needle-to-collector distance, etc. can be varied to alter the properties of the obtained scaffold. Finally, 3D bioprinting allows for the production of complex 3D shapes.[56] In 3D bioprinting, a biomaterial is mixed with cells and functional components to form a bioink. This ink can then be used to directly print structures with encapsulated cells. Murphy and Atala published a review discussing 3D bioprinting as a tool for regenerative medicine.[56] In the context of corneal endothelial tissue engineering, the use of this technique has only been reported once by Kim *et al.* where they used a bioink containing engineered human corneal endothelial cells and a gelatin matrix, while the bioink was directly printed on decellularized amniotic membrane. Unfortunately, this paper provides no further information concerning mechanical properties, thickness, transparency nor permeability and will therefore not be further discussed in this review.[57]

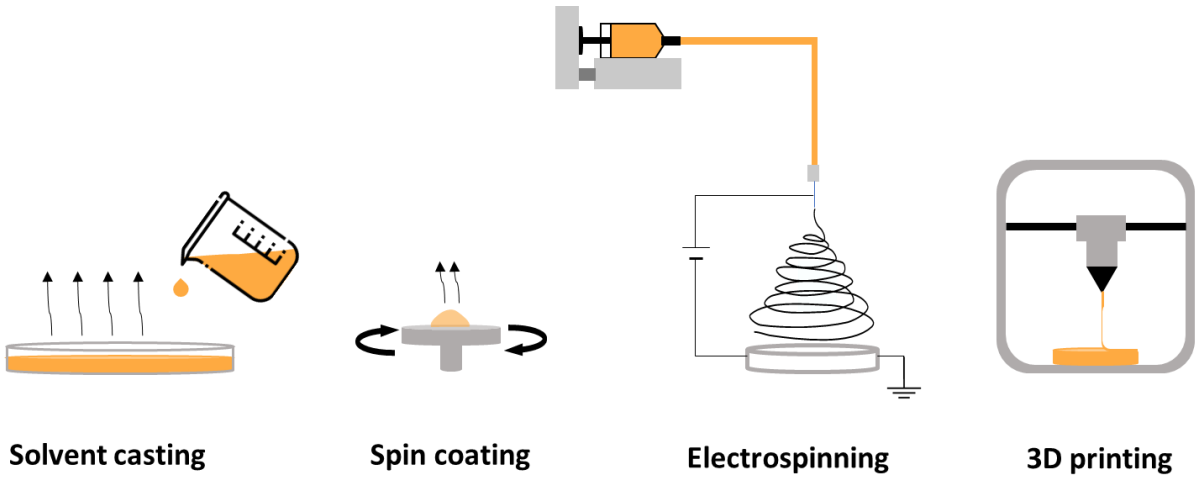

Figure 3. The four most abundantly used polymer processing techniques to produce membranes for corneal tissue engineering; solvent casting, spin coating, electrospinning and 3D printing.

In the following paragraph, properties such as, thickness, permeability, transparency and mechanical strength, of a wide range of materials (i.e. polymers and natural tissue) is discussed. Additionally, the topography of existing scaffolds is briefly analysed. If the specifications of a scaffold are not mentioned, it was not reported in the state-of-the-art. The most common abbreviations of the discussed materials can be found in Table 2.

Table 2: abbreviations of the investigated materials and their meaning.

Abbreviation	Meaning
EDC/NHS	1-ethyl-3-(3-dimethyl aminopropyl) carbodiimide hydrochloride/N-hydroxysuccinimide
FNC	Commercial mix of bovine fibronectin, collagen type I and albumin
Gel-MA	Gelatin-methacylamide
Gel-MA-AEMA	Gel-methacrylamide-aminoethylmethacrylate
Gel-NB	Gelatin-norbornene
HECTS	Hydroxyethyl-Chitosan/gelatin/Chondroitin sulfate
PCL	Poly(ε-caprolactone)
PDLLA	Poly(D,L-lactic acid)
PEG	Polyethylene glycol
PLGA	Poly(lactic-co-glycolic acid)
PMMA	Polymethylmethacrylate

3.1. Importance of the scaffold thickness

The thickness of a scaffold will have an influence on the postoperative visual recovery of a patient. DSAEK surgeries have been successfully performed with grafts up to 200 µm thick, which can give insight in the maximum thickness allowed for a synthetic graft. However, based on the analysis and comparison of corneas after DMEK and DSAEK surgery, Rudolph *et al.* have hypothesised that a thinner graft results in a superior visual outcome as long as the implant is robust enough to allow surgical handling.[30] Preferentially, the artificial scaffold has a thickness comparable to that of the natural DM (3-10 µm) so that the removed volume equals the implanted volume. The majority of the researchers who have reported on a material for corneal tissue engineering mention the thickness of their potential implant and these data are visually represented in Figure 4. The scatterplot indicates that consistent reporting about the methods and measuring conditions is lacking since dimensions of samples in the hydrated state, dry state or both are discriminated. In some cases, the authors do not clearly indicate whether or not the substrates are in the dry state. Additionally, multiple methods have been described to determine the thickness of the scaffold including scanning electron microscopy (SEM), optical coherence tomography (OCT), interferometry, etc. These techniques require different sample preparations and measuring environments which renders a pragmatic comparison impossible.

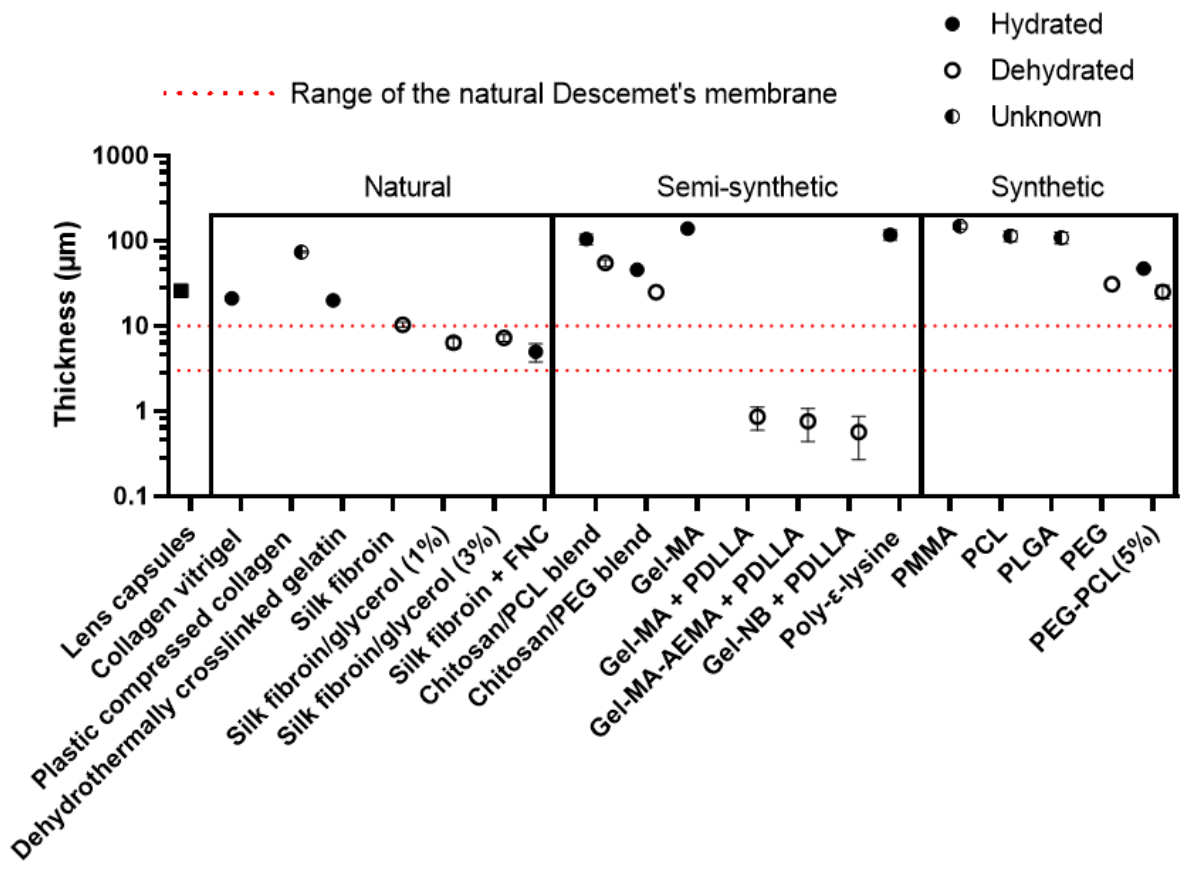

Figure 4. overview of the thickness of scaffolds and materials used in corneal endothelial tissue engineering compared to the thickness of the natural Descemet's membrane (3-10 µm, indicated by the dashed red lines). The squared symbol indicates the thickness of natural tissue (i.e. hydrated lens capsule)

Table 3: overview of thicknesses of natural tissue and natural, semi-synthetic and synthetic scaffolds exploited for corneal endothelial tissue engineering.

Natural Tissue				
Material	**Thickness (µm)**	**Hydrated?**	**Technique**	**Reference**
Human decellularized crystalline lens capsules	25.93 ± 0.26	Yes	OCT	[9]
Natural polymers				
Material	**Thickness (µm)**	**Hydrated?**	**Technique**	**Reference**
Collagen vitrigel	21.2 ± 0.9	Yes	Optical microscope	[58]
Plastic compressed collagen	74.1 ± 2.04	Unknown	OCT	[59]
Dehydrothermally crosslinked gelatin	20	Yes	Microscope	[60]
Silk fibroin	10.39 ± 0.65	No	FE-SEM	[61]
Silk fibroin/glycerol (1%)	6.373 ± 0.86	No		
Silk fibroin/glycerol (3%)	7.25 ± 0.68	No		

Silk fibroin + FNC	5.0 ± 1.2	Yes	Micrometer	[62]
Semi-synthetic polymers				
Material	**Thickness (µm)**	**Hydrated?**	**Technique**	**Reference**
Chitosan/PCL blend	90-120	Yes	Microscope	[63]x
	50-60	No		
Chitosan/PEG blend	26	No	E-SEM	[41]
	25	No	Spectral reflectance	
	46	Yes		
Gel-MA(+)	140	Yes	OCT	[64]x
Gel-MA + PDLLA double layered membrane	0.858 ± 0.262	No	Interferometry	[10]
Gel-MA-AEMA + PDLLA double layered membrane	0.760 ± 0.319	No		
Gel-NB + PDLLA double layered membrane	0.569 ± 0.299	No		
Poly-ε-lysine + ECM proteins	118 ± 16	Yes	Micrometer	[65]
Synthetic polymers				
Material	**Thickness (µm)**	**Hydrated?**	**Technique**	**Reference**
PMMA	150 ± 12	Unknown	Dial Gauge	[66]
PCL	114 ± 16	Unknown		
PLGA	109 ± 17	Unknown		
PEG	31	No	E-SEM	[42]
PEG-PCL (5%)	25.3 ± 4.5	No	Spectral reflectance	
PEG-PCL (5%)	47.2 ± 1.5	Yes	Spectral reflectance	

Figure 4 provides an overview of the thickness of a broad range of samples previously reported in the state-of-the-art. It appears that here natural polymers and semi-synthetic polymers are the best performers, with the first class having four materials that fall in the required thickness range, while the latter has three materials that result in even thinner membranes than the Descemet's membrane. Additionally, comparing the results in this figure and having the final application in mind, the question rises why the thickness in the dry state is reported if the material will be hydrated when applied as a corneal implant. For this reason, the relevance of the reported dimensions solely in the dehydrated state can be questioned. Because the thickness of silk fibroin combined with glycerol in the dehydrated state is similar to that of the DM membrane, the authors conclude that it will be a suitable substrate for corneal endothelial cell regeneration.[61] However, since it has been shown that the swelling ratio of silk in aqueous environments can exceed 1000 %, the thickness will increase during cell seeding and implantation.[67–69] Also Van Hoorick *et al* make this conclusion for their dehydrated scaffolds. However, since the developed membranes have a thickness below 1 µm and include crosslinked gelatin and hydrophobic PDLLA, it is unlikely that the scaffolds will swell up to > 10 µm. For the synthetic polymers PMMA, PCL and PLGA,[67–69] it is unclear if they were measured in the hydrated state but because of their hydrophobic nature, they will only absorb a limited amount of water.

When the thickness in both states is mentioned, the comparison of those values gives an indication of the swelling capacity of the scaffold. From the results of the Chitosan/PCL, Chitosan/PEG and PEG/PCL blend samples, it can be noticed that the fluid uptake of the tissue engineered scaffolds can have a large impact as the thickness is almost doubled from the dry to the hydrated state.[41,42,63] The swelling capacity (S [%]) (equation 3) of hydrogels can also be evaluated based on the degree of swelling, which is calculated by the difference in mass of the hydrogels in the dry (W_d) and in the swollen state (W_h) over the weight in the dry state. The influence of the amount of crosslinking on the degree of swelling of various Gel-MA samples has been investigated by Rizwan *et al.*[64] The results show that the swelling capacity can be drastically reduced upon increasing the amount of crosslinkers.[64] A third method that indicates the water absorption of polymers is the equilibrium water content (W_{eq}) [%] (equation 4). This value is defined as the ratio of the weight difference of samples in the swollen and dry state over the weight in the swollen state.

$$S = \frac{(W_h - W_d)}{W_d} * 100 \quad (3)$$

$$W_{eq} = \frac{(W_h - W_d)}{W_h} * 100 \quad (4)$$

Liang *et al.* did not mention the thickness of their Chitosan-Hydroxyethyl scaffold but only reported the equilibrium water content (i.e. 81.32%).[70] However, determining solely the swelling capacity or equilibrium water content is not enough to evaluate whether membranes will be suitable as DM mimic. The absolute thickness, preferably in the hydrated state, should also be reported. The authors of this review recommend to determine the thickness of the implant in the hydrated state, since the values in the dehydrated state are not representative for the eventual application.

It should be kept in mind that the measuring technique will also have a great influence on the state (dry or hydrated) of the scaffold and the obtained dimensions. Samples for analysis with SEM or field emission SEM (FE-SEM) are required to be dehydrated since a vacuum is applied during the measurement. Therefore, these techniques do not allow the determination of the sample thickness in the hydrated state. With environmental SEM (E-SEM), a specimen can be measured without the need for dehydration, which makes it the SEM technique of choice for the determination of the thickness of DM mimics as discussed in the current review.[71] Optical coherence tomography is a medical imaging technique that is used to obtain a live image of the cross-section of biological tissue in their natural environment, frequently used in ophthalmology to measure retinal or corneal thickness non-invasively. During a DMEK or DSAEK surgery, OCT is for example used to ensure the position of the donor graft in the cornea. However, the determination of the thickness is less precise compared to SEM.[9] To visualise samples with white light interferometry, it is combined with an optical microscope. A disadvantage of this technique is that the light source generates heat, causing water in thin samples such as those made by Van Hoorick *et al.* to evaporate.[10] Therefore, the hydrated thickness is difficult to measure with this device. The dial gauge and micrometer are similar methods which allow to measure sample thickness down to 1 µm accurately. The sample dimensions are determined by placing the object on a stationary anvil after which the spindle is moved until the sample is clamped between the anvil and the spindle. Because of this *modus operandi*, the dial gauge and micrometer are less suitable to determine dimensions of

soft and compressible samples such as scaffolds for corneal endothelial regeneration (i.e. hydrogels).

The overview in Table 3/Figure 4 shows that the thickness of the natural, semi-synthetic and synthetic polymers varies from 5 to 74 µm, 0.6 to 120 µm and 31 to 150 µm respectively. This indicates that it is not straightforward to obtain dimensions comparable to those of the natural DM since only silk fibroin remains within the range of 3-10 µm. Additionally, the results show that especially synthetic materials are difficult to process into very thin membranes as 25.3 µm is the lowest thickness value reported to date (PEG-PCL (5%) in the dehydrated state). The thinnest substrates are the double layered membranes consisting of a PDLLA and a modified gelatin layer produced via spincoating. The synthetic PMMA results in the thickest membrane of about 150 µm. It is not specifically indicated in which state this is measured (dry or hydrated) but since the swelling of PMMA in aqueous solvents is only minor, the thickness will still be within the range of a DSAEK graft (100-200 µm).[72] It should be noted that PMMA as such will not be suitable as it showed only low CEnC interactivity.
Overall, the thickness of most scaffolds remains within the range of the DMEK and DSAEK grafts (20-200 µm).

3.2. Ensuring sufficient nutrient permeability

A flow of water and nutrients through the Descemet's membrane is essential to serve the function of the corneal endothelium. Therefore, the permeability of the Descemet's membrane mimics needs to be evaluated to assess the suitability of a scaffold. The substrate has to reach a minimum permeability for a certain nutrient in order to be applicable as scaffold for endothelial regeneration. As mentioned earlier, studies on the permeability through a human Descemet's membrane are scarce and a threshold permeability for this tissue has not been reported to date. However, data regarding the permeability of an animal cornea are considered a suitable estimation. Hence, the diffusion of a certain nutrient through the tissue engineered scaffold will be adequate if its diffusion or permeability coefficient exceeds that of the animal DM and endothelium. In Table 4, the nutrient or water permeability of multiple scaffolds is provided. The permeability coefficient (P [cm/s]) is calculated using the following equation (5) with dQ/dt representing the change of the amount of nutrients over time [g/s], A being the surface area of the membrane [cm^2] and C_0 representing the initial nutrient concentration [g/l].

$$P = \frac{\left[\frac{dQ}{dt}\right]}{A * C_0} \quad (5)$$

The diffusion coefficient (D [cm^2/s]) is defined as the permeability coefficient multiplied by the thickness of the scaffold (T [cm]) (equation 6).

$$D = P * T \quad (6)$$

Mostly one or both parameters are used to give an indication of the scaffold permeability. In our conducted literature study, only Kimoto *et al.* reported the permeability of water and bovine serum albumin (BSA) through dehydrothermally crosslinked gelatin after 1 hour as a percental value of 28% and 2% respectively.

Table 4: overview of the permeability of natural tissue and natural, semi-synthetic and synthetic scaffolds for corneal tissue engineering.

Natural tissue				
Material	**Chemical**	**P (cm/s)**	**D (cm^2/s)**	**Reference**
Amniotic membrane	Glucose	4×10^{-5}	4.5×10^{-7}	[73]*
Amniotic membrane + endothelium	Glucose	3×10^{-5}		
Lens capsule	Dextran 3 kDa	9×10^{-6}	1.26×10^{-4}	[74]*
	Dextran 10 kDa	3×10^{-6}	7.7×10^{-5}	
	Dextran 40 kDa	1×10^{-6}	5.1×10^{-5}	
	Dextran 150 kDa	1×10^{-6}	4.5×10^{-5}	
Natural polymers				
Material	**Chemical**	**P (cm/s)**	**D (cm^2/s)**	**Reference**
3% dendrimer crosslinked collagen	Glucose		$0.8\text{-}1.1 \times 10^{-6}$	[75]
2% dendrimer crosslinked collagen	Glucose		2.2×10^{-6}	
Semi-synthetic polymers				
Material	**Chemical**	**P (cm/s)**	**D (cm^2/s)**	**Reference**
Chitosan/PEG blend	Glucose		1.0×10^{-6}	[41]
	Bovine Serum Albumin (BSA)		1.0×10^{-8}	
Heparin-modified gelatin crosslinked with EDC/NHS (EDC/amine =5)	FITC-Dextran 4 kDa	$(2.36 \pm 5) \times 10^{-6}$	$(7.78 \pm 1.6) \times 10^{-8}$	[76]
	FITC-Dextran 70 kDa	$(11.3 \pm 1.1) \times 10^{-8}$	$(3.7 \pm 0.4) \times 10^{-9}$	
Gel-MA(+)	BSA	2.2×10^{-7}		[64]
	Glucose	2.7×10^{-5}		
Gel-MA(+) + endothelium	Glucose	$3.4\text{-}4.23 \times 10^{-6}$		
Gel-MA (DS 95) + PDLLA double layered membrane	Glucose	$(2.36 \pm 1.9) \times 10^{-2}$	$(2.03 \pm 1.75) \times 10^{-6}$	[10]
Gel-MA (DS 63) + PDLLA double layered membrane	Glucose	$(3.06 \pm 1.51) \times 10^{-2}$	$(1.91 \pm 1.12) \times 10^{-6}$	
Gel-MA-AEMA + PDLLA double layered membrane	Glucose	$(9.35 \pm 0.885) \times 10^{-3}$	$(7.10 \pm 6.72) \times 10^{-6}$	
Gel-NB + PDLLA double layered membrane	Glucose	$(2.55 \pm 2.47) \times 10^{-2}$	$(2.99 \pm 2.18) \times 10^{-6}$	
HECTS blend	Glucose	1.93×10^{-5}		[70]
Synthetic polymers				
Material	**Chemical**	**P (cm/s)**	**D (cm^2/s)**	**Reference**
PEG-PCL	Glucose		$(2.3 \pm 0.3) \times 10^{-6}$	[42]
	BSA		$(1.0 \pm 0.2) \times 10^{-7}$	
PDLLA	Glucose	$(1.52 \pm 0.619) \times 10^{-2}$	$(8.87 \pm 3.62) \times 10^{-7}$	[10]

*. Data from paper not related to corneal endothelial tissue engineering

Table 4 indicates that mainly the diffusion of glucose and albumin are reported. Nutrients with lower molar masses are mostly not investigated. Indeed, if the permeability of a large molecule reaches a threshold value, it is anticipated that the diffusion of a smaller component will also be sufficient. This is validated by the diffusion coefficient of glucose which is always higher than that of albumin through the same material. Also the permeability of dextran through the lens capsule decreases with increasing molecular weight.
Glucose, which is the main nutrient for corneal cells, diffuses from the anterior chamber towards the stroma, where it undergoes anaerobic metabolization to lactic acid, which diffuses back to the aqueous humour.[77] Therefore, it is valuable to determine the glucose permeability or diffusion coefficient and compare it to values found in literature to assess whether the scaffold is suitable. However, albumin (66.5 kDa) is also present in the stroma and in CEnCs but not in the Descemet's membrane. [78,79] It has already been reported that albumin enters the cornea via the limbal blood vessels instead of through the Descemet's membrane.[78,80–82] This makes glucose, with its molar mass of 0.18 kDa, one of the largest molecules that should migrate through the Descemet's membrane, which might make BSA not representative for permeability assays.[78,80–82] Scientists most likely anticipated that, since the molecular weight of albumin is 370 times larger compared to that of glucose, the permeability of the latter will be acceptable if the former reaches a minimum permeability coefficient. However, a scaffold might be rejected as corneal endothelial implant based on insufficient permeability of albumin while that of glucose is adequate, but not evaluated. Niu *et al.* investigated the permeability of fluorescently labelled dextran (FITC-dextran) with a molecular weight of 4 versus 70 kDa.[76] Considering the molecular weight of glucose, the permeability of the 4 kDa dextran is sufficient to check the suitability of the scaffold.

Frequently, the permeability of the membrane as such is determined. However, it should be noted that there will be a monolayer of corneal endothelial cells present on the eventual implant. One should clearly discriminate the glucose transport over the endothelial layer and the Descemet's membrane, which can be considered active transcellular transport and passive diffusion respectively. Glucose transporters have been found on both the apical and basolateral side of the corneal endothelial cells, indicating a transcellular glucose flux.[83] The nutrient flow might thus also be influenced by the barrier function of the endothelium. To exemplify, the permeability coefficient of Gel-MA(+), a material where Gel-MA is allowed to form a gel prior to crosslinking, is 6 to 8 times smaller when an endothelium is formed on the surface (Table 4).[64] For heparin-modified gelatin crosslinked with EDC/NHS on the other hand, the P and D values were not significantly changed by seeding CEnCs on top, indicating that the membrane is the limiting factor for the permeability.[76]

The synthetic mimic of the Descemet's membrane should be equally or more permeable towards certain nutrients compared to the natural membrane. Since there exist only limited data on the permeability through the Descemet's membrane in literature, the diffusion coefficient of the total cornea for glucose and albumin (D_{cornea} (glucose) = $3.0 \pm 0.2 \times 10^{-6}$ cm^2/s and D_{cornea} (albumin) = 1×10^{-7} cm^2/s) are used as reference values. However, since the thickness of the DM mimic will greatly influence the diffusion capacity, it is recommended to consider the permeability coefficient, which takes the dimensions of the membrane into account, to investigate the suitability of the scaffold. With the average thickness of the cornea (550 µm), the permeability coefficients can be calculated via equation 4 and are found to be

P_{cornea} (glucose) = 6 x 10^{-6} cm/s and P_{cornea} (albumin) = 1 x 10^{-7} cm/s. The amniotic membrane has a P(glucose) which is lower compared to the cornea which indicates that the glucose permeability is insufficient to be a suitable substitute. However, P could be increased by using a thinner membrane. For the Chitosan/PEG blend, the diffusion of BSA also appears to be too low but since the diffusion of glucose is as required, the material can still be an adequate implant. The permeability of (semi-)synthetic membranes can be increased by inducing porosity during the production with e.g. porogens or a laser. Because of its hydrophobicity, PDLLA has a lower permeability for glucose compared to the reference value but combined with gelatin (as is foreseen in the eventual application), the permeability is sufficient. The permeability of dextran through the corneal endothelium should be at least 8.1 ± 1.4 x 10^{-8} cm/s, which is the case for every membrane in Table 4 for which dextran has been screened. It can be concluded that the majority of the scaffolds investigated until now fulfill the requirements regarding the permeability, indicating that this will not be the most challenging demand to reach.
The authors of this review propose to measure the permeability coefficient of glucose through the membrane and compare these to values found in literature, if reported. This is sufficient to investigate if the DM mimic will limit the transport of the nutrients.

3.3. Techniques and materials to ensure a sufficiently transparent scaffold

While transparency of the substrate is by no means essential for correct cellular growth or for the functioning of the tissue carrier, it is, however, essential when considering the final outcome of the transplantation. Especially for non-degradable scaffolds, maximal transparency is a must when the goal is to eventually restore the vision of the patient to pre-disease levels. When looking at the existing scaffolds (Table 5), it is noticeable that most of them are sufficiently transparent and reach or exceed the transparency of the natural Descemet's membrane (>90%). The only exceptions are membranes prepared through electrospinning. These membranes are noticeably opaque compared to scaffolds produced by other processing techniques. While the relevant papers do not report whether transparencies were measured using hydrated or dry membranes, the hydrophobic nature of the considered polymers makes it unlikely that measuring in hydrated or dry state makes much difference. Indeed, upon hydrating electrospun PCL membranes, transparency does not improve. This opaqueness is probably caused by scattering due to the presence of a multitude of randomly oriented polymer fibres in the scaffolds.
On the other hand, hydrogels processed using electrospinning and measured in the hydrated state are expected to be much more transparent than their hydrophobic counterparts, due to the transparent nature of the materials themselves, as well as due to similar diffractive indices between the hydrated polymer and water. A point of critique to be given to the qualitative determinations of transparency, where the membrane or film is placed on a paper with printed letters is that this gives an overestimation of the quality of the image and thus the transparency of the membrane. When positioning films or membranes further from the paper, the letters become increasingly difficult or even impossible to read. This is again most noticeable for electrospun membranes while more homogenous membranes are much less or not limited by this at all. Therefore, qualitative investigation of transparency should also be performed at a fixed distance from the subject, similar to the real situation. In addition, this will give a better

indication of what the quantitative measurement means, since scattered light can for example still be detected by a UV-VIS detector but does not necessarily give a clear image.

When considering techniques used to determine the transparency of the membranes, it becomes clear that UV-VIS photospectroscopy is the preferred method, ideally measuring a continuous spectrum of the visual region (380-750nm).[76] One group also used a lux meter to determine the transparency. This method, however, does not provide information about specific wavelengths and is therefore discouraged.[84] In addition, the authors recommend avoiding electrospinning as a processing technique for this purpose, given its inferior transparencies, especially when employing more hydrophobic polymers. Instead, techniques that produce a more homogeneous membrane, such as spincoating or solvent casting, should be employed. Moreover, amniotic membrane and silk fibroin also perform suboptimal compared to other materials. While degradation of these membranes might over time allow complete transparency as the membranes disappear, the ideal membrane should perform well on both short and long term.

Table 5: overview of the transparencies of natural tissue and natural, semi-synthetic and synthetic scaffolds used in corneal endothelial tissue engineering.

Natural tissue				
Material	**Transparency (%)**	**Wavelengths (nm)**	**Notes**	**Ref**
Amniotic membrane	60-85	400-700		85*
Lens capsule	90	405, 450, 490, 530, 630		9
Natural polymers				
Material	**Transparency (%)**	**Wavelengths (nm)**	**Notes**	**Ref**
Dendrimer crosslinked collagen	>80%-95	390-780		75
Collagen vitrigel	>85	380-700		86
Silk Fibroin	84[+]	380-780		61
Silk Fibroin/glycerol (1%)	82	380-780		
Silk Fibroin/glycerol (3%)	69	380-780		
Silk Fibroin + FNC	98±1.4	500		62
Semi-synthetic polymers				
Material	**Transparency (%)**	**Wavelengths (nm)**		**Ref**
Heparin-modified gelatin crosslinked with EDC/NHS	>95	400-750		76
HECTS blend	>90	400-800		70
Gel-MA(+)	90-92	VIS		64
Gel-MA + PDLLA double layered membrane	>97	380-780	Hydrated	10
	>90	380-780	Dehydrated	
Gel-MA-AEMA + PDLLA double layered membrane	>97	380-780	Hydrated	
	>90	380-780	Dehydrated	
Gel-NB + PDLLA double layered membrane	>97	380-780	Hydrated	
	>90	380-780	Dehydrated	
Chitosan/PCL blend	>97	White light	25% PCL, decreases with	84

			increasing PCL content	
Chitosan/PEG blend	>95	VIS		[41]
PCL/Collagen blend	79[†]	400-800	Electrospun, radial fibres	[87]
Poly-ε-lysine	99.08	460-600		[65]
Synthetic polymers				
Material	**Transparency (%)**	**Wavelengths (nm)**		**Ref**
PCL	14.7 ± 1.9	380-780	Electrospun	[66]
PLGA	5.5 ± 1.3	380-780	Electrospun	
PMMA	2.8 ± 4.1	380-780	Electrospun	
PDLLA	>94	380-780		[10]
PEG-PCL	>98	400-700	Independent of PCL content	[42]

*Found in paper not specifically related to corneal endothelial tissue engineering

[†]Calculated from optical intensity using: $T=100*10^{-A}$ with T being transmission (%) and A being the optical intensity or absorbance.

3.4. Necessity of biodegradability

When a material can be disintegrated in a natural environment by the micro-organisms or enzymes present there without the production of toxic degradation products, it is considered biodegradable.[88] Ideally, the degradation products are excreted from the body via natural pathways. In general, tissue-engineering aims to repair, replace or regenerate tissue or organs by combining a biocompatible scaffold with suitable cells for the application.[89] In this way, a bioartificial tissue is created. When the goal is to permanently replace tissue or organs, the scaffold should not be biodegradable in the implanted environment since it should remain intact for the lifetime of the patient. However, if regeneration or repair of the target is required, it could be desired that the implant degrades over time while being replaced with native tissue.[90] In this case, the degradation time of the implant should match the regeneration or repair time of the natural tissue which should be taken into account during the production of the scaffold. To assess whether or not the materials used for the Descemet's membrane mimic should be degradable, two factors should be considered; degradation rate of the cell support in the anterior chamber and the rate of regeneration of the natural Descemet's membrane.

The Descemet's membrane is a basement membrane consisting of extracellular matrix proteins produced by CEnCs.[91] After implantation in the patients cornea, it is anticipated that the natural Descemet's membrane can be regenerated by the CEnCs that are part of the implant and therefore, the main focus of corneal endothelial tissue engineering has been on the production of biodegradable scaffolds.[10] Currently, human trials with these types of implants have not been performed yet so this assumption has not been verified and the exact regeneration rate of the human DM remains undetermined. It is known that the DM has a thickness of 3 µm at birth and increases to around 10 µm over lifetime which indicates a rather slow growth. Scientists who are trying to develop a suitable degradable scaffold can only estimate the regeneration rate based on animal studies. Medeiros and Sampaio *et al.* removed a disk of corneal endothelial cells from rabbit corneas and compared the healing process with

that of corneas of which a disc of both the corneal endothelium and Descemet's membrane were cut out.[92,93] After one month, the corneal oedema that developed in the first group was already resolved while it took 6 months to restore the injury in the endothelium-DM complex of the second group. This shows that the DM as such exhibits a poor potential to regenerate but that CEnCs on an intact DM can be restored relatively fast.[19] However, this animal model is not fully representing the mechanisms in the human body since, unlike the human CEnCs, rabbit corneal endothelial cells have the capacity to regenerate. Furthermore, the results of the study might be different if the removed endothelium and DM were replaced with a cell-containing scaffold. This renders the estimation of the regeneration rate of the DM and thus the degradation rate of the scaffold difficult.[64] Additionally, it is not certain that a tissue-engineered scaffold that is considered biodegradable, will effectively degrade over time. The eye is an immune privileged organ in which an inflammatory response is rarely triggered.[94] Biodegradability is therefore not an essential requirement for a suitable implant. If the tissue engineered membrane fulfils all requirements and is biostable, a non-biodegradable material will also be applicable. The development of the biomatrix will be easier since the degradation does not have to be considered. The only non-biodegradable polymer that was evaluated in this review is PMMA.[64]

Only the minority of the studies addressed in the current review investigated the degradability of the materials they used (Table 6). Based on the environment in which the degradation was assessed, three different types of degradation studies can be distinguished: hydrolytic degradation in HCl, *in vitro* degradation in the presence of enzymes, aqueous humour or in PBS solution and *in vivo* degradation. The accelerated hydrolytic degradation in acidic environment is performed to generate the degradation products of the material and assess their toxicity. It should be kept in mind that the degradation products obtained with HCl will probably not be the same as those generated *in vivo* but they will be similar. Fibroblasts incubated in the presence of the degradation products of chitosan/PEG blends and PEG-PCL proliferated in the same way as the control, indicating that the products were not toxic.
Two studies investigated material degradation in a collagenase solution. However, this is not representative for the *in vivo* situation since the enzyme is not present in the aqueous humour. This is illustrated by Gel-MA(+) which degraded much faster in a high concentration collagenase solution than in the aqueous humour of a rabbit. Indeed, the aqueous humour and PBS solution mimic the natural environment of the DM to a superior extent. The *in vitro* degradation of PEG-PCL (in PBS solution at 35°C for 8 weeks) showed that the degradation slowed down with increasing PCL content. This can be attributed to the hydrophobic nature of PCL and allows the tunability of the degradation rate which is desirable for tissue engineering. A chitosan/PEG sample was incubated in an L-cysteine and lysozyme mixture at concentrations that exceeded those of the human aqueous humour 100 times. During crosslinking of the blend with cystamine, disulphide bridges are incorporated that can act as additional degradation points for the two enzymes in the environment. This indicates that also the degradation time of chitosan/PEG can be controlled by altering the PEG content.
The deterioration of both hydroxyethyl chitosan and Gel-MA(+) have been observed after implantation in the anterior chamber of rabbits. For the latter, the only indication of degradation after 4 months was the slight increase in pore size, showing that the degradation goes much slower *in vivo* than in the *in vitro* test with aqueous humour.

Table 6. Overview of the degradation properties of natural, semi-synthetic and synthetic scaffolds used for corneal endothelial tissue engineering.

Natural tissue				
Material	**Complete degradation***	**Environment**	**Remarks**	**Reference**
Human decellularized crystalline lens capsules	13 hours	Collagenase (5 U/ml)		[9]
Amniotic membrane	13 hours			
Semi-synthetic polymers				
Material	**Complete degradation***	**Environment**	**Remarks**	**Reference**
Chitosan/PEG blend	50% degradation in 55 days	L-cysteine and lysozyme (1.1 and 6.4 mg/ml respectively)	Cystamine as crosslinker introduces disulphide bridges which act as additional degradation points	[41]
		HCl (370 mg/ml)	Accelerated degradation to assess the toxicity of degradation products.	
Hydroxyethyl Chitosan	60 days	Implanted in skeletal muscles of rats		[95]
	>3 weeks	Implanted in anterior chamber of rabbits	Almost complete degradation of the membrane	
Gel-MA	20 hours	Collagenase (20 U/ml)		[64]
Gel-MA(+)	48 hours			
Gel-MA(+)	22% degradation in 7 days	Aqueous humour from rabbits		
Gel-MA(+)		Implanted in anterior chamber of rabbits	Increased pore size after 4 months as sign of degradation	
Synthetic polymers				
Material	**Complete degradation***	**Environment**	**Remarks**	**Reference**
PEG-PCL (0%)	24% in 8 weeks	PBS solution at 35°C		[42]
PEG-PCL (5%)	15% in 8 weeks			
PEG-PCL (10%)	10% in 8 weeks			
PEG-PCL		HCl (36.5 mg/ml)	Accelerated degradation to assess the toxicity of degradation products.	

*indicates the time necessary for complete degradation in the given environment unless mentioned otherwise.

3.5. Optimizing the cellular response and handleability by tuning the mechanical properties

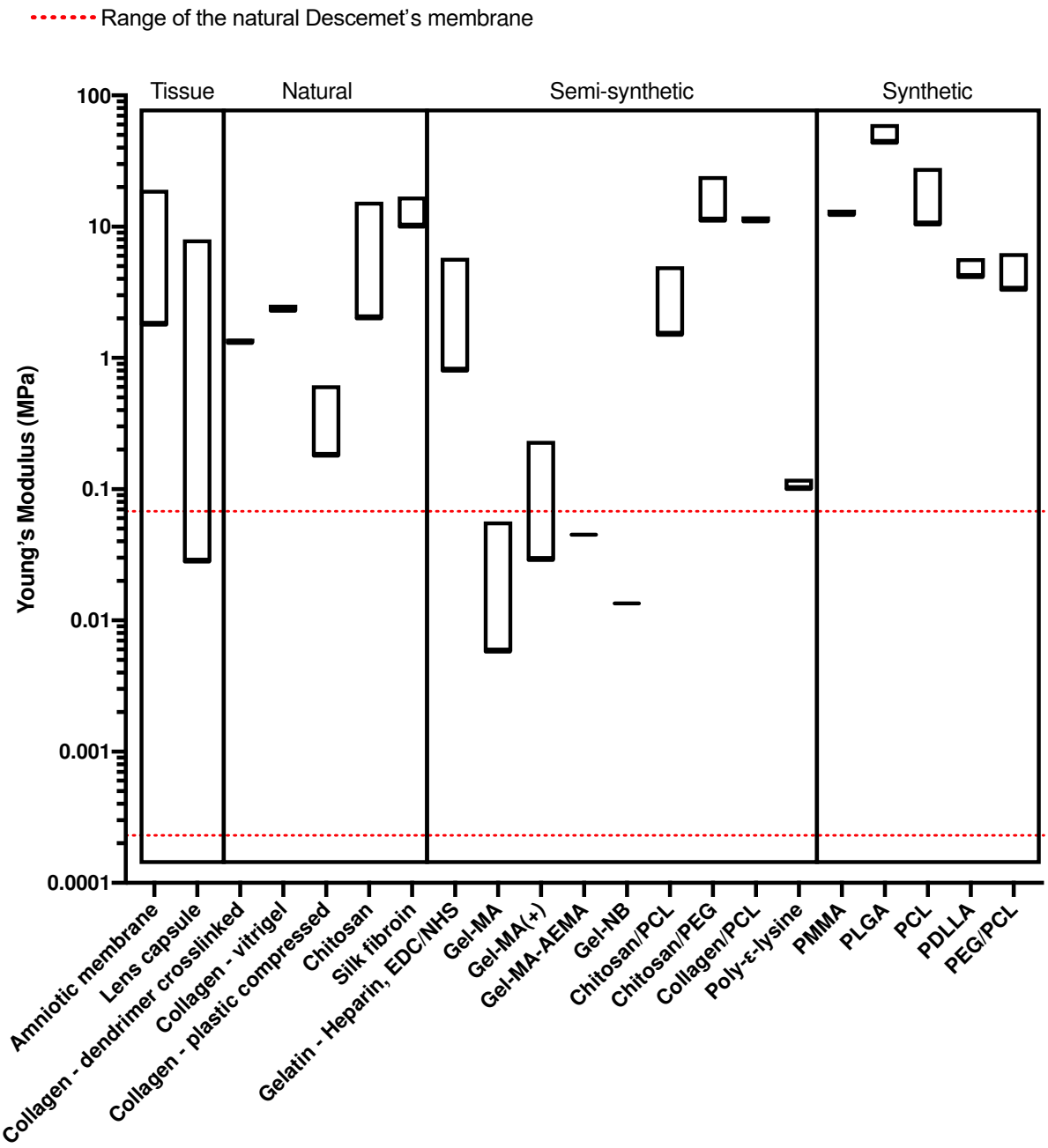

Figure 5. overview of the Young's moduli of scaffolds and materials used in corneal endothelial tissue engineering compared to the Young's modulus of the hydrated natural Descemet's membrane.

An overview of the mechanical properties of the different scaffolds is given in Table 7, while a more concise comparison of the Young's moduli is provided in Figure 5.

The mechanical properties of the Descemet's membrane mimics are both crucial for the surgical handling and with regard to the cellular response. For the former, membranes need to be strong enough to withstand the stresses imposed on the materials during transplantation, here, it was already mentioned in section 2 that the thicker DSAEK membranes provide an improved handleability during the surgical procedure even though it provides a less good

outcome than the thinner DMEK membrane. However, artificial Descemet's membrane can still maintain a good handleability with thinner by selecting more robust materials.
As mentioned earlier, the mechanical properties of the artificial Descemet's membrane will also play a role in the cellular response. Palchesko *et al.* tested materials with various Young's moduli and with various coatings.[96] In their findings, they conclude that a material with a Young's modulus of 50 kPa provoked the best response from the corneal endothelial cells. Stiffer materials (≥830 kPa) showed minimal expression of ZO-1, one of the hallmark proteins for a functioning corneal endothelium. Similar results were found for substrates that were too soft (5 kPa).[96] In hindsight, these results might not be surprising considering a Young's modulus of more or less 50 kPa is very similar to the Young's modulus of the natural Descemet's membrane. This also supports the hypothesis that mimicking the Descemet's membrane to the greatest extent possible will eventually result in a scaffold with the best possible outcome.
When determining the mechanical properties of a material or a scaffold, it is important to take note whether the sample is measured in the dry or hydrated state. While this distinction might be less relevant for hydrophobic polymers, it is increasingly important with increasing hydrophilicity of the scaffold since water will greatly influence the mechanical properties of the material. Typically, hydrogels will exhibit a lower Young's modulus when hydrated and will show a larger peak strain at a lower peak stress compared to their dry state. [,49] Additionally, measurements in the hydrated state will be more relevant since they reflect the conditions in place during cell expansion and in the eye.
Finally, also the processing method might have an influence on the mechanical properties of the material. This is for example the case for electrospun membranes characterized by aligned fibres. In general, these membranes will be stronger when stretched in the direction of the fibres, with a higher Young's modulus and a higher ultimate strength.[97]

Unfortunately, comparing mechanical properties between different papers and materials proves to be troublesome. Often different properties of a material are tested and when similar characteristics are evaluated, the methodology differs significantly, making comparisons dubious at best. Therefore, the authors suggest using a tensile testing apparatus on membranes in the hydrated state. At the very least, the Young's modulus should be determined and preferably also the stress and strain at break should be reported since they more accurately represent the stresses that a membrane will be able to endure and its likeliness to tear.

Table 7: overview of the mechanical properties of natural, semi-synthetic and synthetic scaffolds used for corneal endothelial tissue engineering.

Natural tissue						
Material	**Young's modulus (MPa)**	**Strain at break (%)**	**Stress at break (MPa)**	**Method**	**Notes**	**Reference**
Amniotic membrane	1.79-19.08	-	-	Tensile	Hydrated & partially dried	[98]*
Lens capsule	0.028-8	50 ± 18	2.3 ± 0.7	Various	-	[99]*
Natural polymers						
Material	**Young's modulus (MPa)**	**Strain at break (%)**	**Stress at break (MPa)**	**method**	**Notes**	**ref**

Dendrimer crosslinked collagen	1.4 ± 0.1	-	-	Tensile, 50% humidity	-	[75]
Collagen vitrigel	2.41 ± 0.14	10-30	0.67-13.5	Tensile	-	[100,101]*
Plastic compressed collagen	0.4 ± 0.22	-	-	Tensile	-	[102]*
Chitosan	2500-3500	4-6	60-85	Tensile	Dehydrated	[63]
	2-15.5	37-67	1-9.9	Tensile	Hydrated	[41,63]
Silk fibroin	10-17	4-26	300-740	-	-	[103,104]*
Semi-synthetic polymers						
Material	**Young's modulus (MPa)**	**Strain at break (%)**	**Stress at break (MPa)**	**Method**	**Notes**	**Reference**
Heparin-modified gelatin crosslinked with EDC/NHS	0.8-5.8	127.0-42.3	0.7-1.7	Tensile	EDC/amine ratio 2.5-10.0	[76]
Gel-MA	5.8-56.7 x 10^{-3}	-	-	Compression	10-30wt/V% gelatin	[64]
Gel-MA(+)	28.8-233.3 x 10^{-3}	-	-	Compression	10-30 wt/V% gelatin	
Gel-MA DS97	18 x 10^{-3}	-	-	Rheology		[10]
Gel-MA-AEMA	45 x 10^{-3}	-	-	Rheology		
Gel-NB	13.5 x 10^{-3}	-	-	Rheology		
Chitosan/PCL blend	1.5-5	20-80	0.5-2.2	Tensile	25-75% PCL	[63]
Chitosan/PEG blend	17.7 ± 6.6	101	28.2	Tensile	Hydrated, properties at break correlated with PEG content	[41]
Hydroxyethyl Chitosan	-	18-23	33-41	Tensile	-	[95]*
PCL/Collagen blend	11-12±1	-	-	Tensile	-	[87]
Poly-ε-lysine	0.11 ± 0.01	-	0.04 ± 0.004	Tensile	-	[65]
Synthetic polymers						
Material	**Young's modulus (MPa)**	**Strain at break (%)**	**Stress at break (MPa)**	**Method**	**Notes**	**Reference**
PMMA	12.9 ± 0.6	40	-	Tensile	Electrospun	[105]*
PLGA	52 ± 8.5	73	2.1 ± 0.32	Tensile	Electrospun	[106]*
PCL	2.9-440	170-1000	10	Tensile	-	[63,107,108]*
	23-28	-	3.5	Tensile	Electrospun, parallel to fibres	[97]*

	10.4	-	1.5	Tensile	Electrospun, perpendicular to fibres	[97]*
PDLLA	4.95 ± 0.81	-	-	Tensile	-	[10]
PEG-PCL	3.3-6.3	33-71	1.5-5.2	Tensile	Hydrated	[42]

*Found in paper not specifically related to corneal endothelial tissue engineering

When looking at the Young's modulus of the different materials, it is clear that none of the synthetic materials fall into the range of the hydrated Descemet's membrane (Figure 5), with values that are at least an order of magnitude higher. For the natural materials on the other hand, only the lens capsule seems to overlap with the Young's modulus of the Descemet's membrane. However, the most valuable polymer class for this seems to be semi-synthetic materials, especially gelatin-based. Gel-MA, Gel-MA-AEMA and Gel-NB all fall within the range of Young's moduli of the Descemet's membrane and poly-ε-lysine is just outside the target range. However, one must keep in mind that more materials might have a Young's modulus into the required range when they are hydrated.
When taking a look at blended materials, it seems that their Young's modulus depends on the formulation of the blend. Targeting a certain Young's modulus should thus be possible by selecting an appropriate blend composition. Another method to obtain a scaffold that is both sufficiently strong for handling and is at the same time optimal for cellular growth might be multilayered membranes. Here, a softer hydrogel material might be used as a cell-interactive layer while a stronger material can be used as a supporting layer to provide the necessary strength. This method might be especially relevant for thinner membranes, where soft, hydrogel materials might not provide the needed strength. A similar approach was reported by Van Hoorick *et al.*[10]

3.6. Influence of the scaffold topography on the cellular response

While it was previously discussed that the natural Descemet's membrane appears to be porous, it seems that the topography of artificial membranes also has an influence on the cellular response. While most membranes produced are flat without any distinguishable surface patterns or features, some researchers modified their membranes with certain topographies. Additionally, even though they are suboptimal when considering transparency, certain techniques such as electrospinning allow the production of a defined structure with aligned fibres, which also seems to have an influence on the cellular response. For example, when electrospun fibres are radially aligned, superior proliferation of corneal endothelial cells was observed compared to randomly aligned fibres.[87] This influence might be related to the presence of aligned collagen fibres in the infant Descemet's membrane and might be the preferred environment for cellular expansion. Similarly, Salehi et al. observed cell alignment when using aligned, electrospun poly(glycerol sebacate)/PCL blends.[109] The influence of the membrane topography on the cells is also evident from a paper by Rizwan *et al.* Here, the authors produced patterned Gel-MA films and concluded that the topography of the films has an influence on the expression of both ZO-1 and Na^+/K^+-ATPase, with patterned films showing higher expressions of both, compared to unpatterned membranes.[64] This research indicates that while homogeneous, flat membranes seem to support cells sufficiently, it might also be interesting to look into producing patterns in or on the surface of the membranes to improve

the cellular response. While textures do indeed increase the cellular response *in vitro,* it still remains to be seen if this also results in an actual advantage over non-textured membranes in *in vivo* situations. On the other hand, it has been shown that very pronounced surface irregularities on fish scale derived scaffolds impeded the growth of corneal endothelial cells.[11] Besides having membranes with texture or aligned fibres, several authors have made use of hemispherical or curved membranes.[58,60,62,87] While this is not strictly necessary to have a functioning implant, the hemispherical shape might have a better fit to the posterior side of the cornea.

While the number of papers reporting on textured scaffolds for transplantation purposes is limited to date, an increasing amount of research has been devoted to the application of textured substrates to guide cell growth without the intention to transplant the substrate. An example of this has been reported by Gutermuth *et al.* They exploited two-photon polymerisation to produce polydimethylsiloxane substrates that mimic the texture of the natural Descemet's membrane. Therefore, decellularized Descemet's membrane was scanned to obtain the necessary topological data. Their substrate was able to induce the differentiation of human mesenchymal stromal cells to endothelial-like cells.[110] A recent review by Formisano *et al.* also provides a more in depth discussion about the influence of nanotextured scaffolds on the cultivation of corneal endothelial cells for endothelial regeneration.[111]

3.7. Markers for cellular characterization

Herein, we have reviewed a set of physical and biochemical properties of corneal endothelial cell scaffolds that are being developed for corneal endothelial tissue engineering. However, it has been known that for instance material structure and mechanical properties can influence the cell geno- and phenotype.[112] Therefore, looking at cellular response reflects the propensity of the material to act as a decent endothelial cell scaffold. However, to date there is still no consensus on a unique set of markers that indicate properly grown corneal endothelial cells.[112] Since the pump-and-leak mechanism is attributed to the corneal endothelium as its primary function, markers related to this function are used for characterization. Na^+/K^+-ATPase and ZO-1, responsible for their pump and leak function respectively, are the most cited markers for human corneal endothelial cells. However, they are far from unique. Additionally, the hexagonal cell morphology and size are frequently used properties that are taken into account when tissue engineering a corneal endothelium, either qualitatively or quantitatively.

However, to fully qualify certain material properties of scaffolds, one must evaluate the whole as a tissue rather than the cellular response to the material characteristics.[113] Assays that functionally evaluate the cell-scaffold complex as a tissue are limited and not so frequently implemented. By measuring the transendothelial electrical resistance, the electrical potential over the endothelium is determined.[77] This value reflects the ionic permeability of the endothelium which is crucial to establish the ionic gradient *in vivo* to avoid corneal oedema. In addition, permeability to nutrients and waste products should be evaluated on this tissue level, since the endothelial cells, with the tightness of the zonula occludens, are the regulating factor in the process.[10,23]

4. Conclusions and future perspectives

The data in this review indicate that there is no consistent method to evaluate the properties of tissue engineered scaffolds for corneal endothelial regeneration. The different measuring techniques and conditions give results that are unsuitable for comparison and can lead to unjustified conclusions regarding the suitability of the implant. The authors of this review propose the following measuring conditions. The thickness should be measured in the hydrated state, preferably with OCT, E-SEM or spectral reflectance. For the permeability, the permeability coefficient of glucose should be evaluated. To assess this property, there is a need for permeability studies of glucose through a natural DM with and without corneal endothelial cells to generate consistent benchmark values and to quantitatively determine the contribution of the DM to glucose permeability. The material should also be hydrated when determining the mechanical properties, including the stress and strain at break and the Young's modulus, with a tensile tester. To evaluate these characteristics, pre-set values for the natural DM should be made available since the current ranges are too broad to draw any conclusions. Additionally, transparencies should be determined using photospectroscopy in the visual range (380 - 780 nm). This preferably also in the hydrated state, albeit not strictly necessary for techniques that produce a homogeneous film (e.g. film casting instead of electrospinning).

The overview provided herein also shows that a broad range of materials have already been reported as potential substrate for corneal endothelial regeneration. When natural tissue is investigated for this application, the properties of the materials as such are rarely assessed. Only for the lens capsule, all characteristics criticized in this review were reported. Frequently, a biological evaluation is immediately performed on these materials. It would be beneficial if also of the natural tissues, the thickness, permeability, transparency and mechanical properties would be determined, since these will also be crucial for the success of the graft. The use of natural tissue as substrate also has some disadvantages over polymers. It should be considered that membranes such as the lens capsule are not unlimitedly available. Additionally, because of their origin, the properties of these scaffolds can be variable which makes that the scaffolds will not behave in a predictable way and result in a more complicated surgical procedure with less successful outcomes. An example of this can be found in an article by Hopkinson *et al.* They investigated the inter- and intramembrane variability of transforming growth factor – beta (TGF-β1) in the amniotic membrane. Their results make it clear that natural membranes are highly variable, even when looking at different sections of a single membrane.[114] Additionally, the risk of disease transfer remains. These hurdles are also troubling the current treatment methods involving donor corneas (DMEK and DSAEK). From this point of view, the synthetic DM mimics are appealing since they eliminate all these limitations.

Considering the properties discussed above, it can be concluded that producing a substrate with a thickness comparable to or lower than that of the DM (3-10 µm) shows to be difficult but dimensions in the range of DMEK and DSEAK grafts are manageable and can be obtained using commonly available processing techniques such as spin coating, electrospinning and solvent casting. The minimal permeability was reached for almost every scaffold and can be altered for the (semi-)synthetic substrates by changing the porosity, which indicates that it will not be challenging to fulfil this requirement. For the semi-synthetic and synthetic scaffolds,

only the transparencies of those produced via electrospinning were insufficient, showing that most of these materials are suitable as corneal implant in this regard. The transparency of the natural membranes and most of the scaffolds made from natural polymers on the other hand is ≤ 90%, which is lower compared to the threshold value. In case of the natural polymers, the processing method to obtain the membranes can be changed in an attempt to increase the transparency but for natural tissue, little can be done to increase transparency. Based on this characteristic, the lens capsule and the amniotic membrane cannot be considered suitable scaffold materials. The main hurdle for most substrates remains the mechanical properties. Here a balance needs to be found to obtain a material that is easily handleable while still maintaining good mechanical properties for the cells - two demands that require opposite characteristics of a material - especially when the thickness requirements are taken into account. One way to tackle this problem is through the use of multi-layered membranes where two separate materials can be used to fulfil each of the requirements, resulting in a construct that is optimized for cellular proliferation, thin and handleable. We anticipate that a lot of improvements will still need to be made in this field.
These results are promising but, ideally, all requirements should be fulfilled which is still challenging. Additionally, it should be kept in mind that the important properties are interdependent. Altering the thickness for example will influence the permeability and the mechanical characteristics of a scaffold. However, additional processing steps or more complex scaffold designs show great promise to allow for all requirements to be met.

It could be concluded that membranes constructed from multiple layers show the most promise to fulfill all requirements. More specifically, they allow the combination of properties which are not possible to achieve when using a single material. Strong materials, such as PDLLA or chitosan could be used as a structural layer to obtain a strong membrane while maintaining thicknesses comparable to that of the natural Descemet's membrane. A soft hydrogel on the other hand could be used as an additional layer serving as an extracellular matrix mimic. Especially gelatin-based materials seem to be of interest since their Young's modulus is closest to that of the natural DM and will allow for optimal cell proliferation. Additionally, a combination of different techniques might prove to be beneficial. Spin coating could for example be exploited for the structural layer since it enables the production of the thinnest membranes while solvent casting could be used to create the cell-interactive layer and a textured mold could provide topographical cues to the cells. This combination of techniques would ensure a thin, transparent, strong and permeable membrane that allows for optimal cell response. Therefore, we propose that future research focusses on combining multiple materials to obtain a scaffold that fulfills all requirements. Additionally, more research is needed with regard to the influence of the surface topography on the cells, employing more advanced techniques such as two- photon polymerization or nano-thermoforming which might be beneficial for the production of scaffolds with complex topographies. Furthermore, the degradation behavior and time of the substrate should be considered in the evaluation process. The biodegradation of the materials should be assessed *in vitro* in an environment that is representative for the implantation site (e.g. aqueous humour, PBS solution,…) instead of in the presence of collagenase. A degradable implant should be characterized by a degradation time that meets the regeneration time of the natural DM. However, reports on the *in vivo* regeneration of human DM is scarce which makes it difficult to extract a reference value from literature. Once human trials for corneal tissue engineering commence, valuable data on the regeneration of the natural DM will be gathered and the research will gain momentum. Currently, the main focus was on designing a biodegradable membrane yet also biostable

materials could serve as suitable DM mimics. It is anticipated that this polymer type will find its entry in the field in the future. In practice, the alternative cell therapy treatment with corneal endothelial cell injection is already in a more advanced stage but this method is associated with some limitations. The guttae on the DM, which impede CEnCs growth, are for example not 100% removed which would be the case with the tissue engineered implant discussed herein. Furthermore, using an *ex vivo* grown endothelium, we can control the endothelial cell density, which is not manageable with a cell injection, that relies on cell sedimentation. Therefore, it is still valuable to explore this method further. We hope to see future research explore past the *in vitro* phase with animal trials and maybe even preliminary human trials.

Acknowledgements

L. De Vos and J. Delaey would like to express their gratitude towards the Research Foundation Flanders (FWO) for their financial support during the project (grant number 1S25422N and 1SA2121N). Additionally, P. Dubruel and B. Van den Bogerd would like to thank the FWO for their support through project G059419N.

Bibliography

1 S. R. Flaxman, et al., *Lancet Glob. Heal.*, 2017, **5**, e1221–e1234.

2 R. Pineda, in *Foundations of Corneal Disease*, Springer International Publishing, Cham, 2020, pp. 299–305.

3 B. Van den Bogerd, S. N. Dhubhghaill, C. Koppen, M. J. Tassignon and N. Zakaria, *Surv. Ophthalmol.*, 2018, **63**, 149–165.

4 S. Gandhi and S. Jain, *Keratoprostheses Artif. Corneas Fundam. Surg. Appl.*, 2015, **37**, 19–25.

5 P. Gain, R. Jullienne, Z. He, M. Aldossary, S. Acquart, F. Cognasse and G. Thuret, *JAMA Ophthalmol.*, 2016, **134**, 167–173.

6 J. D. Desautels, M. Moshirfar, T. Martheswaran, K. M. Shmunes and Y. C. Ronquillo, *Ophthalmol. Ther.*, 2020, **9**, 371–379.

7 R. S. Birbal, S. N. Dhubhghaill, L. Baydoun, L. Ham, V. Bourgonje, I. Dapena, S. Oellerich and G. R. J. Melles, *Cornea*, 2020, **39**, 277–282.

8 S. Kinoshita, N. Koizumi, M. Ueno, N. Okumura, K. Imai, H. Tanaka, Y. Yamamoto, T. Nakamura, T. Inatomi, J. Bush, M. Toda, M. Hagiya, I. Yokota, S. Teramukai, C. Sotozono and J. Hamuro, *N. Engl. J. Med.*, 2018, **378**, 995–1003.

9 B. Van den Bogerd, S. Ní Dhubhghaill and N. Zakaria, *J. Tissue Eng. Regen. Med.*, 2018, **12**, e2020–e2028.

10 J. Van Hoorick, J. Delaey, H. Vercammen, J. Van Erps, H. Thienpont, P. Dubruel, N. Zakaria, C. Koppen, S. Van Vlierberghe and B. Van den Bogerd, *Adv. Healthc. Mater.*, 2020, 2000760.

11 M. Parekh, B. Van Den Bogerd, N. Zakaria, D. Ponzin and S. Ferrari, *Stem Cells Int.*, , DOI:10.1155/2018/8146834.

12 N. Koizumi, N. Okumura and S. Kinoshita, *Exp. Eye Res.*, 2012, **95**, 60–67.

13 T. H. van Essen, D. L. Roelen, K. A. Williams and M. J. Jager, *Prog. Retin. Eye Res.*, 2015, **46**, 84–110.

14 J. Vendomèle, Q. Khebizi and S. Fisson, *Front. Immunol.*, , DOI:10.3389/fimmu.2017.01686.

15 M. M. Jumblatt, D. M. Maurice and J. P. McCulley, *Investig. Ophthalmol. Vis. Sci.*, 1978, **17**, 1135–1141.

16 W. Arras, H. Vercammen, S. Ní Dhubhghaill, C. Koppen and B. Van den Bogerd, *Front. Med.*, 2021, **8**, 1–10.

17 B. Van Den Bogerd, N. Zakaria, S. Matthyssen, C. Koppen and S. Ní Dhubhghaill, *Stem Cells Int.*, , DOI:10.1155/2020/5891393.

18 J. F. Jameson, M. O. Pacheco, H. H. Nguyen, E. A. Phelps and W. L. Stoppel, *Bioengineering*, 2021, **8**, 161.

19 R. C. de Oliveira and S. E. Wilson, *Exp. Eye Res.*, 2020, **197**, 108090.

20 S. G. Levy, J. Moss, H. Sawada, P. J. C. Dopping-Hepenstal and A. C. E. McCartney, *Curr. Eye Res.*, 1996, **15**, 45–52.

21 A. Kabosova, D. T. Azar, G. A. Bannikov, K. P. Campbell, M. Durbeej, R. F. Ghohestani, J. C. R. Jones, M. C. Kenney, M. Koch, Y. Ninomiya, B. L. Patton, M. Paulsson, Y. Sado, E. H. Sage, T. Sasaki, L. M. Sorokin, M.-F. Steiner-Champliaud, T.-T. Sun, N. SundarRaj, R. Timpl, I. Virtanen and A. V Ljubimov, *Investig. Opthalmology Vis. Sci.*, 2007, **48**, 4989.

22 D. H. Johnson, W. M. Bourne and R. J. Campbell, *Arch. Ophthalmol.*, 1982, **100**, 1942–1947.

23 J. H. Kim, K. Green, M. Martinez and D. Paton, *Exp. Eye Res.*, 1971, **12**, 231–238.

24 D. Myung, K. Derr, P. Huie, J. Noolandi, K. P. Ta and C. N. Ta, *Ophthalmic Res.*,

2006, **38**, 158–63.
25 C. C. Danielsen, *Exp. Eye Res.*, 2004, **79**, 343–350.
26 Y. Ota, S. Mishima and D. M. Maurice, *Invest. Ophthalmol.*, 1974, **13**, 945–9.
27 W. M. Bourne, S. Nagataki and R. F. Brubaker, *Curr. Eye Res.*, 1984, **3**, 509–513.
28 J. A. Last, S. J. Liliensiek, P. F. Nealey and C. J. Murphy, *J. Struct. Biol.*, 2009, **167**, 19–24.
29 G. A. Abrams, S. S. Schaus, S. L. Goodman, P. F. Nealey and C. J. Murphy, *Cornea*, 2000, **19**, 57–64.
30 M. Rudolph, K. Laaser, B. O. Bachmann, C. Cursiefen, D. Epstein and F. E. Kruse, *Ophthalmology*, 2012, **119**, 528–535.
31 I. Bahar, I. Kaiserman, P. McAllum, A. Slomovic and D. Rootman, *Ophthalmology*, 2008, **115**, 1525–1533.
32 K. Wacker, M. Fritz, V. Grewing, P. C. Maier and T. Reinhard, *Cornea*, , DOI:10.1097/ICO.0000000000002583.
33 R. Di Mundo, G. Recchia, M. Parekh, A. Ruzza, S. Ferrari and G. Carbone, *J. Mech. Behav. Biomed. Mater.*, 2017, **74**, 21–27.
34 S. M. Thomasy, V. K. Raghunathan, M. Winkler, C. M. Reilly, A. R. Sadeli, P. Russell, J. V. Jester and C. J. Murphy, *Acta Biomater.*, 2014, **10**, 785–791.
35 E. A. Boettner, *Invest. Ophthalmol. Vis. Sci.*, 1962, **1**, 776–783.
36 B. Van den Bogerd, S. N. Dhubhghaill, C. Koppen, M.-J. Tassignon and N. Zakaria, *Surv. Ophthalmol.*, 2017, 1–17.
37 H. Elhalis, B. Azizi and U. V. Jurkunas, *Ocul Surf*, 2010, **8**, 173–184.
38 A. O. Eghrari, S. A. Riazuddin and J. D. Gottsch, in *Progress in Molecular Biology and Translational Science*, Elsevier Inc., 1st edn., 2015, vol. 134, pp. 79–97.
39 M. C. Kenney, U. Labermeier, D. Hinds and G. O. Waring, *Exp. Eye Res.*, 1984, **39**, 267–277.
40 D. Xia, S. Zhang, E. Nielsen, A. R. Ivarsen, C. Liang, Q. Li, K. Thomsen, J. Ø. Hjortdal and M. Dong, *Sci. Rep.*, 2016, **6**, 4–10.
41 B. Ozcelik, K. D. Brown, A. Blencowe, M. Daniell, G. W. Stevens and G. G. Qiao, *Acta Biomater.*, 2013, **9**, 6594–6605.
42 B. Ozcelik, K. D. Brown, A. Blencowe, K. Ladewig, G. W. Stevens, J. P. Y. Scheerlinck, K. Abberton, M. Daniell and G. G. Qiao, *Adv. Healthc. Mater.*, 2014, **3**, 1496–1507.
43 M. O. Price and F. W. Price, *Curr. Opin. Ophthalmol.*, 2013, **24**, 329–335.
44 K. M. Meek and C. Knupp, *Prog. Retin. Eye Res.*, 2015, **49**, 1–16.
45 B. ter Horst, N. S. Moiemen and L. M. Grover, in *Biomaterials for Skin Repair and Regeneration*, Elsevier Ltd, 2019, pp. 151–192.
46 C. Dong-Woo, L. Jung-seob, J. Jinah, J. Jin Woo, P. Jeong Hun and P. Falguni, in *Organ Printing*, Morgan & Claypool, 2015.
47 M. A. Macchione, D. Aristizabal Bedoya, F. N. Figueroa and M. C. Strumia, *Synthetic and semi-synthetic polymers for pharmaceutical applications*, Elsevier Inc., 2021.
48 M. S. B. Reddy, D. Ponnamma, R. Choudhary and K. K. Sadasivuni, *Polymers (Basel).*, , DOI:10.3390/polym13071105.
49 V. Kulkarni, K. Butte and S. Rathod, *Int. J. Res. Pharm. Biomed. Sci.*, 2012, **3**, 1597–1613.
50 D. Puppi, C. Federica, M. Dash and E. Cheillini, in *Biodegradable Polymers: Processing, Degradation and Applications*, 2011, pp. 545–604.
51 R. N. Palchesko, S. D. Carrasquilla and A. W. Feinberg, *Adv. Healthc. Mater.*, 2018, **7**, 1–18.
52 Q. Wei, N. N. Deng, J. Guo and J. Deng, *Int. J. Biomater.*, , DOI:10.1155/2018/7158621.
53 T. Çaykara, M. G. Sande, N. Azoia, L. R. Rodrigues and C. J. Silva, *Med. Microbiol. Immunol.*, , DOI:10.1007/s00430-020-00660-8.
54 M. Damala and V. Singh, *Corneal Regeneration*, 2019.
55 S. Agarwal, J. H. Wendorff and A. Greiner, *Polymer (Guildf).*, 2008, **49**, 5603–5621.

56 S. V. Murphy and A. Atala, *Nat. Biotechnol.*, 2014, **32**, 773–785.
57 K. W. Kim, S. J. Lee, S. H. Park and J. C. Kim, *Adv. Healthc. Mater.*, 2018, **7**, 1–13.
58 J. Yoshida, A. Oshikata-Miyazaki, S. Yokoo, S. Yamagami, T. Takezawa and S. Amano, *Investig. Ophthalmol. Vis. Sci.*, 2014, **55**, 4975–4981.
59 H. J. Levis, G. S. L. Peh, K.-P. Toh, R. Poh, A. J. Shortt, R. A. L. Drake, J. S. Mehta and J. T. Daniels, *PLoS One*, 2012, **7**, e50993.
60 M. Kimoto, N. Shima, M. Yamaguchi, Y. Hiraoka, S. Amano and S. Yamagami, *Investig. Ophthalmol. Vis. Sci.*, 2014, **55**, 2337–2343.
61 J. E. Song, B. R. Sim, Y. S. Jeon, H. S. Kim, E. Y. Shin, C. Carlomagno and G. Khang, *J. Biomater. Sci. Polym. Ed.*, 2019, **30**, 263–275.
62 P. W. Madden, J. N. X. Lai, K. A. George, T. Giovenco, D. G. Harkin and T. V. Chirila, *Biomaterials*, 2011, **32**, 4076–4084.
63 A. Sarasam and S. V. Madihally, *Biomaterials*, 2005, **26**, 5500–5508.
64 M. Rizwan, G. S. L. Peh, H. P. Ang, N. C. Lwin, K. Adnan, J. S. Mehta, W. S. Tan and E. K. F. Yim, *Biomaterials*, 2017, **120**, 139–154.
65 S. Kennedy, R. Lace, C. Carserides, A. G. Gallagher, D. A. Wellings, R. L. Williams and H. J. Levis, *J. Mater. Sci. Mater. Med.*, 2019, **30**, 1–13.
66 M. Kruse, P. Walter, B. Bauer, S. Rütten, K. Schaefer, N. Plange, T. Gries, S. Jockenhoevel and M. Fuest, *Curr. Eye Res.*, 2018, **43**, 1–11.
67 G. Freddi, G. Pessina and M. Tsukada, *Int. J. Biol. Macromol.*, 1999, **24**, 251–263.
68 X. Yu, L. Wang, B. Xu, P. Wang, M. Zhou, Y. Yu and J. Yuan, *Eur. Polym. J.*, 2021, **150**, 1–10.
69 S. Grabska-Zielinska, A. Sionkowska, K. Reczynska and E. Pamula, *Polymers (Basel).*, 2020, **12**, 13.
70 Y. Liang, W. Liu, B. Han, C. Yang, Q. Ma, W. Zhao, M. Rong and H. Li, *J. Mater. Sci. Mater. Med.*, 2011, **22**, 175–183.
71 Z. Kaberova, E. Karpushkin, M. Nevoralová, M. Vetrík, M. Šlouf and M. Dušková-Smrcková, *Polymers (Basel).*, , DOI:10.3390/polym12030578.
72 P. W. Akers, A. R. J. Nelson, D. E. Williams and D. J. Mcgillivray, *Appl. Surf. Sci.*, 2015, **353**, 829–834.
73 R. Levkovitz, U. Zaretsky, A. J. Jaffa, M. Hod and D. Elad, *Placenta*, 2013, **34**, 708–715.
74 B. P. Danysh, T. P. Patel, K. J. Czymmek, D. A. Edwards, L. Wang, J. Pande and M. K. Duncan, *Matrix Biol.*, 2010, **29**, 228–236.
75 X. Duan and H. Sheardown, *Biomaterials*, 2006, **27**, 4608–4617.
76 G. Niu, J. S. Choi, Z. Wang, A. Skardal, M. Giegengack and S. Soker, *Biomaterials*, 2014, **35**, 4005–4014.
77 J. A. Bonanno, *Exp. Eye Res.*, 2012, **95**, 2–7.
78 D. W. Nees, R. N. Fariss and J. Piatigorsky, *Investig. Ophthalmol. Vis. Sci.*, 2003, **44**, 3339–3345.
79 H. Gong, M. Johnson, W. Ye, R. D. Kamm and T. F. Freddo, *Exp. Eye Res.*, 1997, **65**, 747–756.
80 H. Wiig, *Exp. Eye Res.*, 1990, **50**, 261–267.
81 D. M. Maurice and P. G. Watson, *Exp. Eye Res.*, 1965, **4**, 355–363.
82 P. N. Hale and D. M. Maurice, *Exp. Eye Res.*, 1969, **8**, 205–215.
83 B. E. Mccarey and F. H. Schmidt, *Curr. Eye Res.*, 1990, **9**, 1025–1039.
84 T. H. Young, I. J. Wang, F. R. Hu and T. J. Wang, *Colloids Surfaces B Biointerfaces*, 2014, **116**, 403–410.
85 C. J. Connon, J. Doutch, B. Chen, A. Hopkinson, J. S. Mehta, T. Nakamura, S. Kinoshita and K. M. Meek, *Br. J. Ophthalmol.*, 2010, **94**, 1057–1061.
86 J. Yoshida, S. Yokoo, A. Oshikata-Miyazaki, S. Amano, T. Takezawa and S. Yamagami, *Curr. Eye Res.*, 2017, **42**, 1420–1425.
87 J. I. Kim, J. Y. Kim and C. H. Park, *Sci. Rep.*, 2018, **8**, 1–13.
88 A. Gierej, F. Berghmans, M. Vagenende, A. Filipkowski, B. Siwicki, R. Buczynski, H. Thienpont, S. Van Vlierberghe, T. Geernaert and P. Dubruel, *J. Light. Technol.*, 2019,

37, 1916–1923.
89 L. Di Silvio, in *Tissue Engineering Using Ceramics and Polymers*, 2007, pp. 319–331.
90 H. Ramaraju, R. E. Akman, D. L. Safranski and S. J. Hollister, *Adv. Funct. Mater.*, , DOI:10.1002/adfm.202002014.
91 R. C. de Oliveira and S. E. Wilson, *Exp. Eye Res.*, 2020, **197**, 108090.
92 C. S. Medeiros, P. Saikia, R. C. De Oliveira, L. Lassance, M. R. Santhiago and S. E. Wilson, *Investig. Ophthalmol. Vis. Sci.*, 2019, **60**, 1010–1020.
93 L. P. Sampaio, T. M. Shiju, G. S. L. Hilgert, R. C. de Oliveira, J. R. DeDreu, A. S. Menko, M. R. Santhiago and S. E. Wilson, *Exp. Eye Res.*, 2021, **213**, 108803.
94 M. Parekh, S. Ferrari, C. Sheridan, S. Kaye and S. Ahmad, *Stem Cells Transl. Med.*, 2016, **5**, 258–264.
95 Y. Wan, K. A. M. Creber, B. Peppley and V. T. Bui, *J. Polym. Sci. Part B Polym. Phys.*, 2004, **42**, 1379–1397.
96 R. N. Palchesko, K. L. Lathrop, J. L. Funderburgh and A. W. Feinberg, *Sci. Rep.*, , DOI:10.1038/srep07955.
97 G. H. Kim, *Biomed. Mater.*, 2008, **3**, 25010.
98 J. Benson-Martin, P. Zammaretti, G. Bilic, T. Schweizer, B. Portmann-Lanz, T. Burkhardt, R. Zimmermann and N. Ochsenbein-Kölble, *Eur. J. Obstet. Gynecol. Reprod. Biol.*, 2006, **128**, 103–107.
99 K. S. Avetisov, N. A. Bakhchieva, S. E. Avetisov, I. A. Novikov, A. A. Frolova, A. A. Akovantseva, Y. M. Efremov, S. L. Kotova and P. S. Timashev, *J. Mech. Behav. Biomed. Mater.*, 2020, **103**, 103600.
100 X. Calderón-Colón, Z. Xia, J. L. Breidenich, D. G. Mulreany, Q. Guo, O. M. Uy, J. E. Tiffany, D. E. Freund, R. L. McCally, O. D. Schein, J. H. Elisseeff and M. M. Trexler, *Biomaterials*, 2012, **33**, 8286–8295.
101 X. Wang, J. Maruotti, S. Majumdar, J. Roman, H. Q. Mao, D. J. Zack and J. H. Elisseeff, *J. Tissue Eng. Regen. Med.*, 2018, **12**, 821–829.
102 K. Hu, H. Shi, J. Zhu, D. Deng, G. Zhou, W. Zhang, Y. Cao and W. Liu, *Biomed. Microdevices*, 2010, **12**, 627–635.
103 L. D. Koh, Y. Cheng, C. P. Teng, Y. W. Khin, X. J. Loh, S. Y. Tee, M. Low, E. Ye, H. D. Yu, Y. W. Zhang and M. Y. Han, *Prog. Polym. Sci.*, 2015, **46**, 86–110.
104 N. Johari, L. Moroni and A. Samadikuchaksaraei, *Eur. Polym. J.*, 2020, **134**, 109842.
105 C. Carrizales, S. Pelfrey, R. Rincon, T. M. Eubanks, A. Kuang, M. J. McClure, G. L. Bowlin and J. Macossay, *Polym. Adv. Technol.*, 2008, **19**, 124–130.
106 M. Mehrasa, M. A. Asadollahi, B. Nasri-Nasrabadi, K. Ghaedi, H. Salehi, A. Dolatshahi-Pirouz and A. Arpanaei, *Mater. Sci. Eng. C*, 2016, **66**, 25–32.
107 K. Ragaert, I. De Baere, J. Degrieck and L. Cardon, *6th Polym. Mould Innov. Int. Conf. Proc.*, 2014, 339–344.
108 F. Croisier, A. S. Duwez, C. Jérôme, A. F. Léonard, K. O. Van Der Werf, P. J. Dijkstra and M. L. Bennink, *Acta Biomater.*, 2012, **8**, 218–224.
109 S. Salehi, M. Czugala, P. Stafiej, M. Fathi, T. Bahners, J. S. Gutmann, B. B. Singer and T. A. Fuchsluger, *Acta Biomater.*, 2017, **50**, 370–380.
110 A. Gutermuth, J. Maassen, E. Harnisch, D. Kuhlen, A. Sauer-Budge, C. Skazik-Voogt and K. Engelmann, *Cornea*, 2019, **38**, 110–119.
111 N. Formisano, G. Sahin, P. Català, R. Truckenmüller, R. M. M. A. Nuijts, M. M. Dickman, V. L. S. LaPointe and S. Giselbrecht, *Appl. Sci.*, 2021, **11**, 1–13.
112 B. Van den Bogerd, N. Zakaria, B. Adam, S. Matthyssen, C. Koppen and S. Ni Dhubhghaill, *Transl. Vis. Sci. Technol.*, 2019, **8**, 13.
113 P. Català, G. Thuret, H. Skottman, J. S. Mehta, M. Parekh, S. Ní Dhubhghaill, R. W. J. Collin, R. M. M. A. Nuijts, S. Ferrari, V. L. S. LaPointe and M. M. Dickman, *Prog. Retin. Eye Res.*, , DOI:10.1016/j.preteyeres.2021.100987.
114 A. Hopkinson, R. S. McIntosh, P. J. Tighe, D. K. James and H. S. Dua, *Investig. Opthalmology Vis. Sci.*, 2006, **47**, 4316.